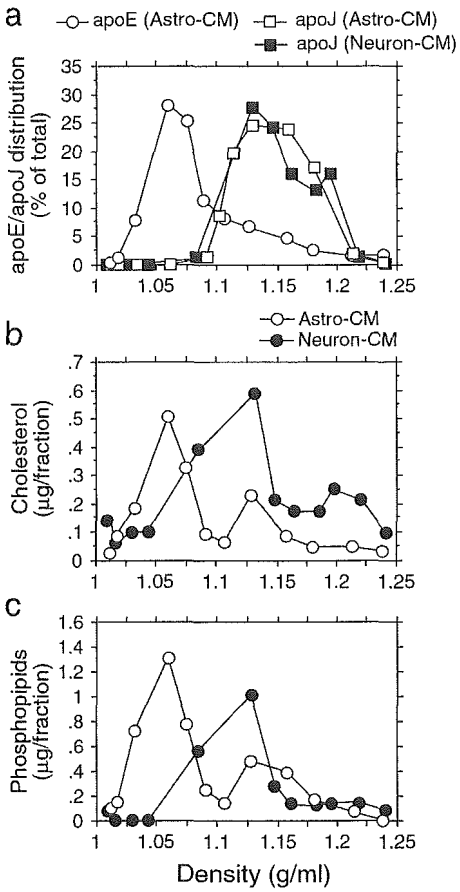

FIG. 5. **Comparison of the distribution pattern of apolipoproteins and lipids in the conditioned media of cultured astrocytes and neurons.** Density gradient ultracentrifugation of the conditioned culture media of neurons was performed to obtain 12 fractions. The neurons were cultured in serum-free N2-supplemented DMEM/F-12 medium (N2 medium) for 2 days, washed with fresh DMEM, and incubated in N2 medium for another 2 days. The culture medium was centrifuged at 1,600 × *g* for 15 min, and the supernatant was collected and subjected to the initial discontinuous density gradient analysis using sucrose solutions as described under "Experimental Procedures." After centrifugation, fractions were collected and analyzed for their cholesterol and phospholipids contents. Aliquots of 10 μl from each fraction were mixed with the same volume of sample buffer and subjected to SDS-PAGE. The separated proteins were immunoblotted with an anti-apoE antibody and an anti-apoJ antibody. No apoE signal was detected in the conditioned culture medium of neurons. The intensities of apoJ signals detected by Western blotting were determined by densitometric analysis as described under "Experimental Procedures." For comparison, the results of the distribution of apoE3 and lipids across the fractions of the conditioned culture media of astrocytes are used. The values of each parameter are expressed in terms of the density of each fraction (*x* axis). The distributions of apoE3 (○) and apoJ (□) across the density of the conditioned culture medium of astrocytes and that of apoJ (■) of the conditioned culture medium of neurons are shown (*a*). The distributions of cholesterol and phospholipids for the astrocyte culture medium are shown as *open circles* (*b* and *c*), and those for neuronal culture medium are shown as *closed circles* (*b* and *c*). *Astro-CM*, the conditioned culture medium of astrocytes; *Neuron-CM*, the conditioned culture medium of neurons.

ated from neurons and astrocytes examined in this study are comparable.

These results indicate that apoE-lipid complexes have isoform-dependent stoichiometry of lipids to apoE. Thus, we next determined the molar and weight ratios of cholesterol and phospholipids to apoE. The quantification of apoE in a given fraction was carried out by Western blot analysis, followed by densitometric analysis using recombinant human apoE3 and apoE4 as standards. As shown in Table I, the molar ratio of cholesterol to apoE with apoE3-lipid particles was 2.1-fold greater than that with apoE4-lipid particles. On the other hand, weight ratio of phospholipids to apoE with apoE3-lipid particles was 2.3-fold greater than that with apoE4-lipid particles. These values are comparable with the difference in the amount of lipids released from apoE3- and apoE4-expressing astrocytes (Fig. 1).

TABLE I

The molar and weight ratios of cholesterol and phospholipids to apoE associated with lipid complex released to cultured media

The culture media of astrocytes expressing human apoE3 or apoE4 were changed to DMEM without serum. The cultures were incubated for 5 days, and then the conditioned media of each culture were collected. The conditioned culture media were fractionated by density gradient ultracentrifugation, and the amounts of cholesterol and phospholipids in the HDL fraction (fraction number 4) were determined as described under "Experimental Procedures." The amount of apoE in the same fraction was determined by quantitative Western blot analysis as described under "Experimental Procedures." ND, not determined.

	Cholesterol/apoE		Phospholipids/apoE	
	Molar ratio	Weight ratio	Molar ratio	Weight ratio
ApoE3	250 ± 6.0	2.85 ± 0.64	ND	5.35 ± 1.28
ApoE4	119 ± 5.1[a]	1.36 ± 0.54[b]	ND	2.37 ± .075[b]

[a] $p < 0.05$ *versus* apoE for triplicate samples.
[b] $p < 0.01$ *versus* apoE for triplicate samples.

These results show that the ability of apoE3 to form lipid particles is greater than that of apoE4, indicating that lipid particles are generated in a stable form by apoE3 with less number of apoE molecules than apoE4. We further determined and compared the sizes of the particles associated with apoE3 and apoE4. The sizes of the apoE-lipid particles in HDL fraction 4 were analyzed by nondenaturing gradient gel electrophoresis. Each sample from the conditioned culture media of the apoE3- and apoE4-expressing astrocytes was separated by electrophoresis and subsequently analyzed by apoE Western blotting (Fig. 6). Two populations of prominent apoE-lipid particles with diameters of 6.3 and 8.97 nm were present in fraction 4 of the conditioned culture medium for both apoE3- and apoE4-expressing astrocytes. Equivalent amounts of aliquots were used for Western blot analysis with an anti-apoJ antibody, and no signal was detected (data not shown). The apoE-lipid particle sizes were determined by calculation of the size of each band based on the size standards. The particle sizes of the apoE3-expressing astrocytes are similar to those of apoE4-expressing astrocytes (Table II).

It has been suggested that disulfide-linked dimeric apoA-II exhibits stronger ability to promote lipid release than monomeric apoA-II because of its increased number of helical segments (44). Because apoE3 contains cysteine at residue 112 and apoE4 does not, the higher ability of apoE3 to promote lipid release may be caused by its increased number of helical segments due to the formation of disulfide-linked dimers. To examine this possibility, we performed immunoblot analysis of the conditioned culture media of apoE3- and apoE4-expressing astrocytes under reducing and nonreducing conditions. In the absence of β-mercaptoethanol, the conditioned culture media of apoE3-expressing astrocytes contained oligomers, mainly dimers and less amount of tetramers, in addition to monomers, whereas those of apoE4-expressing astrocytes contained monomers (Fig. 7*a*). Obviously, the band representing apoE3 dimer was higher than the expected one (M_r = 68,400). Because it is known that serum apoE3 forms homodimers that migrate anomalously on SDS gel under nonreducing conditions (45), this may also be the case for apoE3 dimer in the conditioned culture media. The oligomers found in the conditioned culture media of apoE3-expressing astrocytes were found to be monomers, when the samples were incubated with 10% β-mercaptoethanol (Fig. 7*b*).

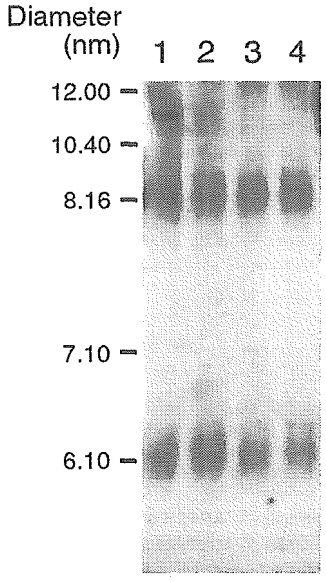

FIG. 6. **Native and nondenaturing gradient gel electrophoresis of apoE3- and apoE4-expressing astrocyte lipoprotein particles followed by Western blot analysis.** ApoE-rich fraction 4 from each conditioned culture media of apoE3- and apoE4-expressing astrocytes, under nondenaturing and nonreducing conditions, was electrophoresed on a nondenaturing 4–20% TBE gradient gel, followed by Western blot analysis using an anti-apoE antibody. Amersham Biosciences native high molecular weight standards were used for hydrated diameter assessment. *Lanes 1* and *2*, samples from fraction 4 of different conditioned culture media of apoE3-expressing astrocytes; *lanes 3* and *4*, samples from fraction 4 of different conditioned culture media of apoE4-expressing astrocytes. Four independent experiments showed similar results.

TABLE II

Particle size of apoE-lipid complex in the conditioned culture media of mouse astrocytes expressing human apoE3 or apoE4

The conditioned culture media of astrocytes expressing human apoE3 and apoE4 were concentrated 5-fold using Centriprep-10 (Millipore, Bedford, MA) prior to fractionation. Two milliliters of the HDL fraction (fraction number 4) was further concentrated to 200 μl using Centricon YM10 (Millipore). The samples were electrophoresed on a nondenaturing 4–20% gradient gel, and the separated proteins were transferred onto a polyvinylidene difluoride membrane (Millipore) and probed with an anti-apoE antibody, AB947. As shown in Fig. 6, apoE associated with HDL-like particles was visualized as separated bands, and the sizes were determined in comparison with the migration of the standard proteins of known diameters (HMW calibration kit, Amersham Biosciences). There was no significant difference in the size of lipid particles obtained between apoE3- and apoE4-expressing astrocytes. $n = 3$ for each sample.

ApoE genotype	Particle size; diameter (nm)	
	Small	Large
ApoE3	6.30 ± 0.01	8.97 ± 0.02
ApoE4	6.31 ± 0.01	8.97 ± 0.02

DISCUSSION

Here, we demonstrate the apoE isoform-dependent lipid release from cultured astrocytes prepared from apoE3 and apoE4 knock-in mice. Although we have found no apoE isoform-dependent differences in size between the apoE3 and apoE4 lipid particles, nor in the total amount of released apoE between apoE3 and apoE4 astrocytes, the apoE3-specific enhancement of lipid release from the cells was observed. These results indicate that apoE3 has a higher ability to generate apoE lipid particles with less numbers of apoE molecules per particle than apoE4, suggesting that apoE3-expressing astrocytes could supply more cholesterol to neurons than apoE4-expressing astrocytes, thereby supporting neuronal plasticity and promoting neuronal regeneration.

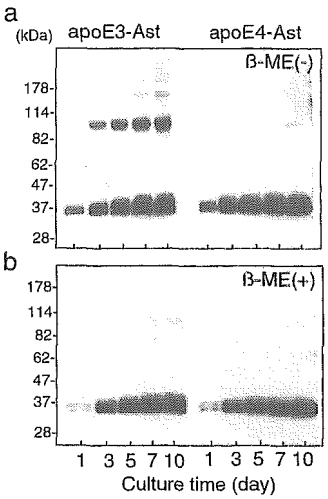

FIG. 7. **Time course of apoE release into the conditioned medium from cultured apoE3- and apoE4-expressing astrocytes.** Shown are the results of Western blot analysis under nonreducing or reducing conditions of apoE3 and apoE4 in the conditioned culture medium of apoE3- and apoE4-expressing astrocytes, respectively. Oligomeric apoE (mainly dimers and less amount of tetramers) was found in the samples of apoE3-expressing astrocyte cultures, but not in those of apoE4-expressing astrocyte cultures (*a*). When the samples were incubated in Laemmli buffer containing 10% β-mercaptoethanol (*β-ME*), such oligomers were not detected in both samples (*b*). Five independent experiments show similar results.

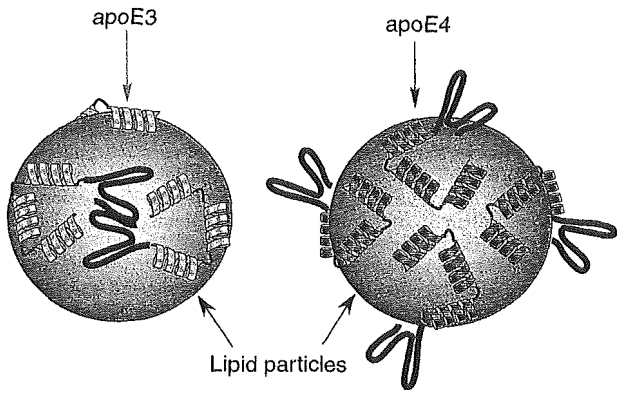

FIG. 8. **Model of apoE lipid particles generated by apoE3- and apoE4-expressing astrocytes.** The present data indicate that apoE3 has the ability to generate similarly sized apoE lipid particles with less number of apoE molecules than apoE4. Based on these findings, we propose a model showing that one apoE4-containing lipid particle contains ~2-fold numbers of apoE molecules compared with an apoE3-containing lipid particle.

It was reported that apolipoproteins with multiple α-helix segments of 20–30 amino acid residues, in which hydrophobic and hydrophilic residues are aligned on opposite sides of the axis, induce cholesterol efflux from cells when added to the culture medium (44, 46–50). ApoE is one of such apolipoproteins, and the effects of apoE on cholesterol release have been examined in various cell systems (51–54). This apolipoprotein-mediated cholesterol release results in the generation of pre-β-HDL, which contains apolipoproteins, cellular cholesterol, and phosphatidylcholine. Recent studies (31, 37) have demonstrated that HDL-like particles in association with exogenous or endogenous apoE are also generated in the cultured medium of the central nervous system cells such as astrocytes and neurons. In addition, we have found that the addition of exogenous apoE promotes lipid release from the central nervous system cells generating HDL-like particles in an apoE isoform-dependent manner (34). Consistent with our previous findings using exogenous apoE, the present study also shows that the

amount of lipids released from apoE3- and apoE4-expressing astrocytes is apoE isoform-dependent, with the order of potency being apoE3 > apoE4. However, the mechanism underlying this isoform-dependent cholesterol release remains undetermined.

Therefore, the next question to be addressed is what is the mechanism underlying the apoE isoform-dependent cholesterol release. We found that the amount of lipids released from apoE3-expressing astrocytes is ~2.5-fold greater than that from apoE4-expressing astrocytes, whereas the amount of apoE3 released is similar to that of apoE4. One possible explanation to this may be that each particle contains equal amount of apoE proteins; however, particles containing apoE3 contain ~2.5-fold greater amounts of lipids than those containing apoE4. Another possible explanation may be that each particle contains equal amounts of lipids, but apoE3-containing particles contain lower numbers of apoE molecules than apoE4-containing particles. This implies that apoE3 has the ability to form lipid particles with a lower number of apoE molecules than apoE4, and thus to generate ~2.5-fold greater numbers of apoE-lipid particles than apoE4 with the same number of apoE molecules. Between these two possibilities, our experiment favors the latter because, as shown in Fig. 6 and Table II, the sizes of particles in both conditioned culture media of apoE3- and apoE4-expressing astrocytes are similar.

The apoE isoform-dependent difference in the association of lipoprotein particles may be explained in terms of the mechanism underlying the apoE isoform-specific formation of apoE oligomers; apoE3 protein forms dimers, and apoE4 does not. This difference may be because apoE3 has cysteine at position 112 of the N-terminal domain, whereas apoE4 has arginine at the same position. Previous studies have shown that the number and the length of amphiphilic helices are responsible for determining the ability of a given apolipoprotein to promote lipid release (44, 49, 55). Interestingly, human apoA-II is known to form disulfide-linked dimers and exhibit stronger ability to promote lipid release than monomeric apoA-II (44). These lines of evidence allow us to postulate that the higher ability of apoE dimers than apoE monomers to promote lipid release may explain the greater amounts of lipids released in the conditioned culture media of apoE3-expressing astrocytes than apoE4-expressing astrocytes. Based on this assumption, we propose a model of the isoform-dependent association of apoE with lipid particles (Fig. 8). Consistent with our present results, previous studies have revealed the conformational adaptability of apoE the N-terminal domain as a function of lipid availability (56) or the presence of competitor apolipoproteins (for review see Ref. 57). In these studies, a model of two possible conformations of apoE on spherical lipid particles was proposed; at a high apoE concentration, the N-terminal domain is displaced from the lipid surface to form a helix bundle in a closed conformation, whereas at a low concentration on the surface, the four helix bundles of the N-terminal domain are in an open conformation, and all the helices are in contact with the lipid surface. Based on these lines of evidence together with our findings that an apoE3-containing HDL-like particle contains approximately one-half the number of apoE molecules compared with an apoE4-containing particle, it may be possible that the apoE isoform-dependent conformational change occurs on the surface of lipid particles; the N-terminal domain of apoE3 is in an open conformation, whereas that of apoE4 is in closed helix bundle conformation.

Another possible explanation may be the preferential association of apoE isoforms with lipoproteins; apoE4 preferentially associates with very low density lipoprotein, whereas apoE3 associates with HDL. This assumption is based on the facts that the N-terminal domain modulates the lipid-binding preference elicited by the C-terminal domain (58, 59) and that the interaction between the N- and C-terminal domains is responsible for this isoform preference (60, 61). It has been suggested that in apoE4, the interaction of arginine 61 with glutamic acid 255 may stabilize an extended helical structure in the carboxyl terminus that is best accommodated on a less curved very low density lipoprotein surface, whereas this interaction does not exist in apoE3, which therefore lacks stability and has shorter helices and preference for HDL (61, 62). Based on these lines of evidence, apoE3 may preferentially bind to an HDL particle with a lower number of apoE molecules to stabilize the particle, whereas apoE4 has less binding efficacy to an HDL particle, which requires higher numbers of apoE molecules to stabilize the particle. Because the physical properties of apoE are assumed to influence its functions (*i.e.* how it associates with lipid particles and stabilizes them), the apoE-isoform-dependent difference in the stability among the 22-kDa N-terminal fragments of apoE (63) may be involved in the isoform-dependent binding efficacy of apoE to HDL particles.

Previous studies (48–50, 54) have demonstrated that various cells generate cholesterol-rich HDL-like particles with exogenous apolipoproteins. However, this is not the case with astrocytes, because we and other researchers have found that generation of HDL by endogenous apoE and by exogenous apoE is differently regulated in cultured astrocytes; HDL-like particles that are generated with exogenous apolipoproteins have low amounts of cholesterol (34, 37), whereas HDL-like particles generated with endogenous apoE are cholesterol-rich (37). In support of these findings, the present study has shown that apoE-lipid particles generated by the endogenously synthesized and released apoE are cholesterol-rich, compared with those generated by the addition of exogenous apoE (34). Because the amount of apoE that is free from lipid particles in the cultured medium and CSF is below detection limit (see Ref. 31 and this study) (Fig. 4, *a* and *b*), these results suggest that under physiological conditions, cholesterol-rich lipid particles associated with endogenous apoE are the major cholesterol source for neurons in the central nervous system. In this regard, it is of interest to note that apoE3-expressing astrocytes could supply more cholesterol in the form of apoE lipid particles to other cells including neurons with comparable levels of apoE secretion than apoE4-expressing astrocytes. Under the steady-state conditions, the lipid metabolisms in the central nervous system appear similar between the brains of apoE3 and apoE4 knock-in mice; the concentrations of free and esterified cholesterol in the postnuclear supernatant, plasma membrane, and endoplasmic reticulum of the brain homogenate are similar (64). However, under different conditions such as during recovery phases after brain injury and cell damage, endogenous apoE-mediated generation of HDL-like particles could play a critical role in cholesterol delivery to neurons, which are an essential material for axonal regeneration and synapse formation (65–68). Actually, previous studies (69, 70) have demonstrated that traumatic brain injury is the most robust environmental risk factor for development of AD. These lines of evidence may allow us to postulate that the apoE isoform dependence of the development of AD may be explained by the apoE isoform-dependent ability in the cholesterol supply to neurons after injury and cell damage, leading to neuroregeneration.

REFERENCES

1. Jarvik, G. P., Wijsman, E. M., Kukull, W. A., Schellenberg, G. D., Yu, C., and Larson, E. B. (1995) *Neurology* **45,** 1092–1096
2. Notkola, I. L., Sulkava, R., Pekkanen, J., Erkinjuntti, T., Ehnholm, C., Kivinen, P., Tuomilehto, J., and Nissinen, A. (1998) *Neuroepidemiology* **17,** 14–20
3. Kivipelto, M., Helkala, E. L., Hanninen, T., Laakso, M. P., Hallikainen, M.,

Alhainen, K., Soininen, H., Tuomilehto, J., and Nissinen, A. (2001) *Neurology* **56,** 1683–1689
4. Wolozin, B., Kellman, W., Ruosseau, P., Celesia, G. G., and Siegel, G. (2000) *Arch. Neurol.* **57,** 1439–1443
5. Jick, H., Zornberg, G. L., Jick, S. S., Seshadri, S., and Drachman, D. A. (2000) *Lancet* **356,** 1627–1631
6. Simons, M., Keller, P., De Strooper, B., Beyreuther, K., Dotti, C. G., and Simons, K. (1998) *Proc. Natl. Acad. Sci. U. S. A.* **95,** 6460–6464
7. Fassbender, K., Simons, M., Bergmann, C., Stroick, M., Lutjohann, D., Keller, P., Runz, H., Kuhl, S., Bertsch, T., von Bergmann, K., Hennerici, M., Beyreuther, K., and Hartmann, T. (2001) *Proc. Natl. Acad. Sci. U. S. A.* **98,** 5856–5861
8. Mori, T., Paris, D., Town, T., Rojiani, A. M., Sparks, D. L., Delledonne, A., Crawford, F., Abdullah, L. I., Humphrey, J. A., Dickson, D. W., and Mullan, M. J. (2001) *J. Neuropathol. Exp. Neurol.* **60,** 778–785
9. Distl, R., Meske, V., and Ohm, T. G. (2001) *Acta Neuropathol.* **101,** 547–554
10. Kakio, A., Nishimoto, S. I., Yanagisawa, K., Kozutsumi, Y., and Matsuzaki, K. (2001) *J. Biol. Chem.* **276,** 24985–24990
11. Czyzewski, K., Lalowski, M. M., Pfeffer, A., and Barcikowska, M. (2001) *Acta Neurobiol. Exp.* **61,** 21–26
12. Roth, G. S., Joseph, J. A., and Mason, R. P. (1995) *Trends Neurosci.* **18,** 203–206
13. Mulder, M., Ravid, R., Swaab, D. F., de Kloet, E. R., Haasdijk, E. D., Julk, J., van der Boom, J. J., and Havekes, L. M. (1998) *Alzheimer Dis. Assoc. Disord.* **12,** 198–203
14. Mason, R. P., Shoemaker, W. J., Shajenko, L., Chambers, T. E., and Herbette, L. G. (1992) *Neurobiol. Aging* **13,** 413–419
15. Howland, D. S., Trusko, S. P., Savage, M. J., Reaume, A. G., Lang, D. M., Hirsch, J. D., Maeda, N., Siman, R., Greenberg, B. D., Scott, R. W., and Flood, D. G. (1998) *J. Biol. Chem.* **273,** 16576–16582
16. Yip, C. M., Elton, E. A., Darabie, A. A., Morrison, M. R., and McLaurin, J. (2001) *J. Mol. Biol.* **311,** 723–734
17. Ji, S.-R., Wu, Y., and Sui, S. F. (2002) *J. Biol. Chem.* **277,** 6273–6279
18. Liu, Y., Peterson, D. A., and Schubert, D. (1998) *Proc. Natl. Acad. Sci. U. S. A.* **95,** 13266–13271
19. Michikawa, M., Gong, J. S., Fan, Q. W., Sawamura, N., and Yanagisawa, K. (2001) *J. Neurosci.* **21,** 7226–7235
20. Gong, J. S., Sawamura, N., Zou, K., Sakai, J., Yanagisawa, K., and Michikawa, M. (2002) *J. Neurosci. Res.,* in press
21. Fan, Q. W., Yu, W., Senda, T., Yanagisawa, K., and Michikawa, M. (2001) *J. Neurochem.* **76,** 391–400
22. Koudinov, A. R., and Koudinova, N. V. (2001) *FASEB J.* **15,** 1858–1860
23. Sawamura, N., Gong, J. S., Garver, W. S., Heidenreich, R. A., Ninomiya, H., Ohno, K., Yanagisawa, K., and Michikawa, M. (2001) *J. Biol. Chem.* **276,** 10314–10319
24. Roheim, P. S., Carey, M., Forte, T., and Vega, G. L. (1979) *Proc. Natl. Acad. Sci. U. S. A.* **76,** 4646–4649
25. Pitas, R. E., Boyles, J. K., Lee, S. H., Hui, D., and Weisgraber, K. H. (1987) *J. Biol. Chem.* **262,** 14352–14360
26. Borghini, I., Barja, F., Pometta, D., and James, R. W. (1995) *Biochim. Biophys. Acta* **1255,** 192–200
27. Weisgraber, K. H., Roses, A. D., and Strittmatter, W. J. (1994) *Curr. Opin. Lipidol.* **5,** 110–116
28. Boyles, J. K., Pitas, R. E., Wilson, E., Mahley, R. W., and Taylor, J. M. (1985) *J. Clin. Invest.* **76,** 1501–1513
29. Nakai, M., Kawamata, T., Taniguchi, T., Maeda, K., and Tanaka, C. (1996) *Neurosci. Lett.* **211,** 41–44
30. Pitas, R. E., Boyles, J. K., Lee, S. H., Foss, D., and Mahley, R. W. (1987) *Biochim. Biophys. Acta* **917,** 148–161
31. LaDu, M. J., Gilligan, S. M., Lukens, J. R., Cabana, V. G., Reardon, C. A., Van Eldik, L. J., and Holtzman, D. M. (1998) *J. Neurochem.* **70,** 2070–2081
32. Beffert, U., Danik, M., Krzywkowski, P., Ramassamy, C., Berrada, F., and Poirier, J. (1998) *Brain Res. Brain Res. Rev.* **27,** 119–142
33. Fan, Q. W., Isobe, I., Asou, H., Yanagisawa, K., and Michikawa, M. (2001) *J. Am. Aging Assoc.* **24,** 1–10
34. Michikawa, M., Fan, Q. W., Isobe, I., and Yanagisawa, K. (2000) *J. Neurochem.* **74,** 1008–1016
35. Fagan, A. M., Holtzman, D. M., Munson, G., Mathur, T., Schneider, D., Chang, L. K., Getz, G. S., Reardon, C. A., Lukens, J., Shah, J. A., and LaDu, M. J. (1999) *J. Biol. Chem.* **274,** 30001–30007
36. Li, Q., Komaba, A., and Yokoyama, S. (1993) *Biochemistry* **32,** 4597–4603
37. Ito, J., Zhang, L.-Y., Asai, M., and Yokoyama, S. (1999) *J. Neurochem.* **72,** 2362–2369
38. Hamanaka, H., Katoh-Fukui, Y., Suzuki, K., Kobayashi, M., Suzuki, R., Motegi, Y., Nakahara, Y., Takeshita, A., Kawai, M., Ishiguro, K., Yokoyama, M., and Fujita, S. C. (2000) *Hum. Mol. Genet.* **9,** 353–361
39. Isobe, I., Michikawa, M., and Yanagisawa, K. (1999) *Neurosci. Lett.* **266,** 129–132
40. Isobe, I., Yanagisawa, K., and Michikawa, M. (2000) *Exp. Neurol.* **162,** 51–60
41. Michikawa, M., and Yanagisawa, K. (1999) *J. Neurochem.* **72,** 2278–2285
42. Laemmli, U. K. (1970) *Nature* **227,** 680–685
43. McCall, M. R., Forte, T. M., and Shore, V. G. (1988) *J. Lipid Res.* **29,** 1127–1137
44. Hara, H., Komaba, A., and Yokoyama, S. (1992) *Lipids* **27,** 302–304
45. Weisgraber, K. H., and Shinto, L. H. (1991) *J. Biol. Chem.* **266,** 12029–12034
46. Mendez, A. J. (1997) *J. Lipid Res.* **38,** 1807–1821
47. Yokoyama, S. (1998) *Biochim. Biophys. Acta* **1392,** 1–15
48. Hara, H., and Yokoyama, S. (1992) *Biochemistry* **31,** 2040–2046
49. Bielicki, J. K., Johnson, W. J., Weinberg, R. B., Glick, J. M., and Rothblat, G. H. (1992) *J. Lipid Res.* **33,** 1699–1709
50. Forte, T. M., Goth-Goldstein, R., Nordhausen, R. W., and McCall, M. R. (1993) *J. Lipid Res.* **34,** 317–324
51. Basu, S. K., Goldstein, J. L., and Brown, M. S. (1983) *Science* **219,** 871–873
52. Huang, Y., von Eckardstein, A., Wu, S., Maeda, N., and Assmann, G. (1994) *Proc. Natl. Acad. Sci. U. S. A.* **91,** 1834–1838
53. Zhang, W. Y., Gaynor, P. M., and Kruth, H. S. (1996) *J. Biol. Chem.* **271,** 28641–28646
54. Hara, H., and Yokoyama, S. (1991) *J. Biol. Chem.* **266,** 3080–3086
55. Segrest, J. P., Jones, M. K., De Loof, H., Brouillette, C. G., Venkatachalapathi, Y. V., and Anantharamaiah, G. M. (1992) *J. Lipid Res.* **33,** 141–166
56. Saito, H., Dhanasekaran, P., Baldwin, F., Weisgraber, K. H., Lund-Katz, S., and Phillips, M. C. (2001) *J. Biol. Chem.* **276,** 40949–40954
57. Narayanaswami, V., and Ryan, R. O. (2000) *Biochim. Biophys. Acta* **1483,** 15–36
58. Sparrow, J. T., Sparrow, D. A., Fernando, G., Culwell, A. R., Kovar, M., and Gotto, A. M., Jr. (1992) *Biochemistry* **31,** 1065–1068
59. De Pauw, M., Vanloo, B., Weisgraber, K., and Rosseneu, M. (1995) *Biochemistry* **34,** 10953–10966
60. Dong, L. M., Wilson, C., Wardell, M. R., Simmons, T., Mahley, R. W., Weisgraber, K. H., and Agard, D. A. (1994) *J. Biol. Chem.* **269,** 22358–22365
61. Dong, L. M., and Weisgraber, K. H. (1996) *J. Biol. Chem.* **271,** 19053–19057
62. Raffai, R. L., Dong, L. M., Farese, R. V., Jr., and Weisgraber, K. H. (2001) *Proc. Natl. Acad. Sci. U. S. A.* **98,** 11587–11591
63. Morrow, J. A., Segall, M. L., Lund-Katz, S., Phillips, M. C., Knapp, M., Rupp, B., and Weisgraber, K. H. (2000) *Biochemistry* **39,** 11657–11666
64. Hayashi, H., Igbavboa, U., Hamanaka, H., Kobayashi, M., Fujita, S. C., Gibson Wood, W., and Yanagisawa, K. (2002) *Neuroreport* **13,** 383–386
65. Poirier, J. (1994) *Trends Neurosci.* **17,** 525–530
66. Posse de Chaves, E. I., Rusinol, A. E., Vance, D. E., Campenot, R. B., and Vance, J. E. (1997) *J. Biol. Chem.* **272,** 30766–30773
67. Posse de Chaves, E. I., Vance, D. E., Campenot, R. B., Kiss, R. S., and Vance, J. E. (2000) *J. Biol. Chem.* **275,** 19883–19890
68. Mauch, D. H., Nagler, K., Schumacher, S., Goritz, C., Muller, E. C., Otto, A., and Pfrieger, F. W. (2001) *Science* **294,** 1354–1357
69. Roberts, G. W., Allsop, D., and Bruton, C. (1990) *J. Neurol. Neurosurg. Psychiatry* **53,** 373–378
70. Nicoll, J. A., Roberts, G. W., and Graham, D. I. (1995) *Nat. Med.* **1,** 135–137

The Journal of Neuroscience, June 15, 2002, 22(12):4833–4841

A Novel Function of Monomeric Amyloid β-Protein Serving as an Antioxidant Molecule against Metal-Induced Oxidative Damage

Kun Zou, Jian-Sheng Gong, Katsuhiko Yanagisawa, and Makoto Michikawa

Department of Dementia Research, National Institute for Longevity Sciences, Obu, Aichi 474-8522, Japan

Aggregated and oligomeric amyloid β-protein (Aβ) is known to exhibit neurotoxicity. However, the action of Aβ monomers on neurons is not fully understood. We have studied aggregation state-dependent actions of Aβ and found an oligomer-specific effect of Aβ on lipid metabolism in neurons (Michikawa et al., 2001). Here, we show a novel function of monomeric Aβ1–40, which is the major species found in physiological fluid, as a natural antioxidant molecule that prevents neuronal death caused by transition metal-induced oxidative damage. Monomeric Aβ1–40, which is demonstrated by SDS-PAGE after treatment with glutaraldehyde, protects neurons cultured in a medium containing 1.5 μM Fe(II) without antioxidant molecules. Metal ion chelators such as EDTA, CDTA (*trans*-1,2-diaminocyclohexane-*N*,*N*,*N*′,*N*′-tetraacetic acid), and DTPA (diethylenetriamine-*N*,*N*,*N*′,*N*″,*N*″-penta-acetic acid, an iron-binding protein, transferrin, and antioxidant scavengers such as catalase, glutathione, and vitamin E also inhibit neuronal death under the same conditions. Monomeric Aβ1–40 inhibits neuronal death caused by Cu(II), Fe(II), and Fe(III) but does not protect neurons against H_2O_2-induced damage. Monomeric Aβ1–40 inhibits the reduction of Fe(III) induced by vitamin C and the generation of superoxides and prevents lipid peroxidation induced by Fe(II). Aβ1–42 remaining as a monomer also exhibits antioxidant and neuroprotective effects. In contrast, oligomeric and aggregated Aβ1–40 and Aβ1–42 lose their neuroprotective activity. These results indicate that monomeric Aβ protects neurons by quenching metal-inducible oxygen radical generation and thereby inhibiting neurotoxicity. Because aggregated Aβ is known to be an oxygen radical generator, our results provide a novel concept that the aggregation-dependent biological effects of Aβ are dualistic, being either an oxygen radical generator or its inhibitor.

Key words: Alzheimer's disease; amyloid β-protein; transition metals; oxygen radicals; antioxidant; neuronal death

One of the neuropathological hallmarks of Alzheimer's disease (AD) is the formation of extracellular amyloid deposits (Selkoe, 1994). The major component of the amyloid deposits is the 39–42 amino acid peptide of the amyloid β-protein (Aβ) (Glenner and Wong, 1984; Masters et al., 1985). One of the Aβ species, ending with a C terminus at residue 40 (Aβ1–40), is the predominant soluble species in biological fluids (Vigo-Pelfrey et al., 1993; Ida et al., 1996). The longer form of Aβ, ending at residue 42 (Aβ1–42), accumulates initially and predominantly in parenchymal plaques (Roher et al., 1993; Iwatsubo et al., 1994). Aβ1–42 is normally produced and secreted by cells in much lower quantities than Aβ1–40, which represents ~90% of the total secreted Aβ. It is believed that aggregated Aβ exerts neurotoxicity and initiates the progressive pathophysiology of AD (Mattson et al., 1993; Pike et al., 1993; Lorenzo and Yankner, 1994; Hartley et al., 1999). However, the function of monomeric Aβ on neurons is not yet fully understood.

It has been reported that the levels of metals such as zinc, iron, and copper are significantly concentrated in senile plaques (Smith et al., 1997; Lovell et al., 1998b). These observations followed original reports showing that these metals promote Aβ aggregation (Bush et al., 1994a,b; Huang et al., 1997; Atwood et al., 1998), which is reversed by treatment with chelators *in vitro* (Huang et al., 1997) and *in vivo* (Cherny et al., 2001). In support of these findings, a recent study has clearly demonstrated that zinc and copper induce non-β-sheeted Aβ aggregation but inhibit β-sheeted aggregation and fibril formation (Yoshiike et al., 2001). Other studies have suggested that accumulated metals support the AD pathology as a possible source of reactive oxygen radicals (Smith et al., 1997; Lovell et al., 1998b; Sayre et al., 2000).

Recent studies showed that the surrounding regions of Aβ deposits in brains of patients with AD and Down's syndrome have no damage (Nunomura et al., 2000, 2001) and that there is an inverse correlation between Aβ burden and the levels of oxidized nucleic acids in the AD brain (Cuajungco et al., 2000b). Although aggregated Aβ is reported to generate free radicals (Hensley et al., 1994; Schubert and Chevion, 1995; Kay, 1997; Huang et al., 1999a; Monji et al., 2001b), these lines of evidence imply a new function of Aβ other than that of a radical generator. A previous report has suggested its antioxidant activity for lipoproteins (Kontush et al., 2001); however, no explanation has been provided as to the mechanism behind the disparate results from different laboratories regarding Aβ-induced oxidative stress versus others suggesting antioxidant properties.

In light of the above, we have studied the aggregation state-dependent actions of Aβ on neurons (Michikawa et al., 2001; Gong et al., 2002). Here, we show that monomeric Aβ1–40 and also Aβ1–42 serve as antioxidant molecules protecting neurons from oxygen radicals generated in a metal-dependent manner, providing new insights into the strategy for developing a therapy for patients with AD.

Received Dec. 3, 2001; revised March 19, 2002; accepted March 22, 2002.

This study was supported by a research grant for Longevity Sciences (H11-001), Research on Brain Science from the Ministry of Health and Welfare, and by Core Research for Evolutional Sciences and Technology, Japan.

Correspondence should be addressed to Dr. Makoto Michikawa, Department of Dementia Research, National Institute for Longevity Sciences, 36-3 Gengo, Morioka, Obu, Aichi, 474-8522, Japan. E-mail: michi@nils.go.jp.

MATERIALS AND METHODS

Reagents and preparation. Synthetic human Aβ1–40 was purchased from Peptide Institute Inc. (Osaka, Japan; lot numbers 510116 and 501001) and Bachem (Bubendorf, Switzerland; lot number 0538913). Aβ40–1 (lot number D539530) was purchased from Bachem, and Aβ1–42 (lot number 510523), Aβ1–16 (lot number 490704), and Aβ25–35 (lot number 500701) were purchased from Peptide Institute Inc. Aβ1–40, Aβ1–42, and Aβ25–35 were dissolved in DMSO at 2 mM and then diluted with distilled water to a concentration of 200 μM. Although the solution was clear, it is known that an Aβ solution contains short fibrils (Naiki et al., 1998). To remove short fibrils, Aβ solutions were centrifuged at 100,000 × *g* for 1 hr at 4°C, using a Beckman Optima TLX table ultracentrifuge and a Beckman TLA-120.2 fixed-angle rotor. Aβ1–16 was directly dissolved in water to a concentration of 200 μM. Oligomeric Aβ1–40 was prepared as described previously (Michikawa et al., 2001). Transferrin, insulin, progesterone, putrescine, selenite, superoxide dismutase (SOD), catalase, glutathione, vitamin E, and vitamin E acetate were obtained from Sigma (St. Louis, MO). The B27 supplement and B27 minus antioxidants (B27-AO) were purchased from Invitrogen (Grand Island, NY). EDTA was purchased from Eastman Kodak Company (Rochester, NY). *trans*-1,2-diaminocyclohexane-*N*,*N*,*N*′,*N*′-tetra-acetic acid (CDTA), diethylenetriamine-*N*,*N*,*N*′,*N*″,*N*‴-penta-acetic acid (DTPA), iron sulfate heptahydrate, iron nitrate nonahydrate, and copper sulfate pentahydrate were obtained from Wako Pure Chemical Industries, Ltd. (Osaka, Japan). Monoclonal antibody, namely, anti-4-hydroxy-2-nonenal (4-HNE) antibody, which recognizes oxidized 4-HNE, was purchased from NOF Corporation (Tokyo, Japan).

Cell culture. All experiments were performed in compliance with existing laws and the institutional guidelines. Cerebral cortical neuronal cultures were prepared from Sprague Dawley rats at embryonic day 17 as described previously (Michikawa and Yanagisawa, 1998). The dissociated single cells were suspended in a feeding medium and plated onto poly-D-lysine-coated 12-well plates at a cell density of 5×10^{-5}. The feeding medium consisted of DMEM/F12 containing 0.1% bovine albumin fraction V solution (Invitrogen) and N2 (Bottenstein and Sato, 1979), B27, or B27-AO supplements.

Quantification of neuron survival. For assessment of cell viability of cultured neurons, phase-contrast photomicrographs were taken before treatment and at various time points after treatment. The number of viable neurons on each micrograph was determined in premarked microscope fields (10× objective). Viable neurons were identified on the basis of morphological criteria. Neurons with intact neurites with uniform diameter and soma with a smooth round appearance were considered viable, whereas neurons with fragmented neurites and shrunken cell bodies were considered nonviable. In a pilot study, cell viability was confirmed by testing cell membrane permeability using propidium iodide (PI) or by staining with a viable cell-specific marker, calcein AM, as described previously (Michikawa and Yanagisawa, 1998). Neurons were stained with Hoechst 33342 (bis-benzamide; 2.5 μg/ml), to visualize their nuclear morphology. Most neurons died during culturing in DMEM/F12 medium supplemented with B27-AO (B27-AO medium) or DMEM/F12 medium supplemented with N2 and $FeSO_4$, $CuSO_4$, or $Fe(NO_3)_3$. For each determination of cell viability, 1000–1400 cells were counted.

Thioflavin-T binding assay for aggregated Aβ. Determination of the aggregated state of Aβ in solution was performed on the basis of a previously established method (LeVine, 1995; LeVine, 1999). The conditioned media, in which the cultures were incubated with Aβ, were collected. Each well contained 50 μl of each medium in 1 ml per well of 5 μM thioflavin-T in 50 mM glycin-NaOH, pH 8.5. Steady-state fluorescence intensities for each sample were determined in 48-well plates with a multiplate reader (Fluoroskan Ascent, Labsystems Inc., Franklin, MA) (excitation 446 nm, emission 490 nm). The culture media to which Aβ was not added were used as the background.

Cross-linking of Aβ with glutaraldehyde. SDS-PAGE of cross-linked fAβ1–40 and iAβ1–40 was performed as described previously (Levine, 1995). Briefly, 8 μg of each peptide in a stock solution (200 μM) was diluted to 35 μl with H_2O. One-tenth volume of glutaraldehyde (3.5 μl of 0.625% diluted from a 25% stock solution) was added to each solution followed by the addition of an excess amount of $NaBH_4$ (10 μl of 0.175 M, 6.6 mg/ml, in 0.1 M NaOH). After 10 min of incubation, 15 μl of the SDS-PAGE sample buffer containing 100 mM dithiothreitol and 20% sucrose was added. Boiling of the amyloid peptides in the sample buffer was avoided, because SDS-resistant multimeric complexes are formed from non-cross-linked peptides during heating in SDS (LeVine, 1995). Then, 20 μl of the mixture was subjected to SDS-PAGE using a 4–20% gradient gel as described previously (Michikawa et al., 2001). The gel was then visualized by silver staining. To compare the aggregation status of Aβ1–40 and Aβ1–42 in 8 mM sodium phosphate, pH 7.4, or DMEM/F12 medium, freshly dissolved Aβ1–40 and Aβ1–42 were incubated at 20 μM for 3 hr at 37°C in each solution. The protein concentration of each solution of Aβ1–40 and Aβ1–42 was determined, 2.8 μg of each peptide was subjected to cross-linking, and the peptides were subjected to electrophoresis and silver staining.

Iron reduction assays. Assays were performed according to a previously reported method (Huang, 1999a). Aβ1–40 (10 μM), Aβ1–42 (10 μM), DTPA (10 and 300 μM) or Fe(III) (25 μM), and 3-(2-pyridyl)-5,6-*bis*(4-sulfo-phenyl)-1,2,4-triazine (PDT) (250 μM) were added to 1 ml of 8 mM sodium phosphate, pH 7.4, and rotated at 25°C for 6 hr. Vitamin C (10 μM) was then added, and the mixture was further incubated at 37°C for 14 hr. A solution containing Fe(III) and Aβ1–40 at the same concentrations in the absence of the indicator PDT was used to determine the background levels of this assay system. The absorbance at 562 nm indicates the amount of reduced iron ion, Fe(II).

Measurement of superoxide levels. The levels of intracellular superoxide anion radicals were measured using hydroethidium (HE), which is oxidized to a fluorescent ethidium cation by superoxides, using methods similar to those described previously (Bindokas et al., 1996). In brief, cells were incubated for 30 min in the presence of 5 μM HE (Molecular Probes, Eugene, OR) at 37°C in 5% CO_2 atmosphere, and confocal images of cell-associated HE fluorescence were acquired (excitation = 488 nm and emission >560 nm).

Western blot analysis for determination of lipid peroxidation. Cerebral cortices of Sprague Dawley rats at embryonic day 17 were isolated and minced with a cutter and incubated in PBS in the presence of 3 or 5 μM Fe(II) with or without fAβ1–40 at 10 μM for 4 hr at 37°C. The fragments were then homogenized in RIPA buffer (150 mM NaCl, 10 mM Tris-HCl, pH 7.5, 1% Nonidet P-40, 0.1% SDS, and 0.25% sodium deoxycholate) and centrifuged at 10,000 × *g* for 10 min at 4°C, and the supernatants were recovered. Protein concentrations of the supernatants were determined by the BCA method (Pierce, Rockford, IL). Western blot analysis was performed according to the methods described previously (Michikawa et al., 2001). In brief, 24 μg of each protein was separated by 4–20% gradient SDS-PAGE and electrotransferred onto nitrocellulose membranes. The membranes were incubated with monoclonal primary antibody, anti-4-HNE antibody, at 2 μg/ml overnight at 4°C. The membranes were then washed in PBS containing 0.05% Tween 20 (PBS-T) three times, followed by incubation with HRP-conjugated goat anti-mouse IgG (1:5000 dilution) for 1 hr at room temperature. The membranes were washed four times in PBS-T and visualized with an ECL kit (Amersham Pharmacia Biotech, Buckinghamshire, UK).

RESULTS

Freshly dissolved Aβ1–40 protects neurons against death induced by antioxidant-depleted medium

We studied the effect of Aβ1–40 on neuronal viability. The medium used was DMEM nutrient mixture (DMEM/F12, 50:50) containing B27-AO. When neurons were incubated in the B27-AO medium, cultured neurons appeared healthy 40 hr after plating; however, neuronal death was induced 48 hr after plating, and most of the cells were dead 64 hr after plating (Fig. 1*a–c*). In contrast, neuronal death was inhibited in the presence of freshly dissolved Aβ1–40 (fAβ1–40) at a concentration of 5 μM 64 hr after plating (Fig. 1*d*). Addition of DMSO at a final concentration of 1% DMSO to the B27-AO medium did not prevent or accelerate neuronal death (Fig. 1*e*). Figure 1*e* shows the time-dependent curves of neuronal viability of the cultures treated with fAβ1–40 at various concentrations. The neuronal death induced by incubation in the B27-AO medium was inhibited by fAβ1–40 in a dose-dependent manner. Neuronal viability was maintained at the initial levels when the cultures were treated with fAβ1–40 at concentrations of 10 and 20 μM until 4 d after the commencement of the treatment (Fig. 1*e*). The neurons at each time point were stained with Hoechst 33342 and PI. The viable neurons at culture day 2 had larger swollen cell bodies (Fig. 1*b*), and the

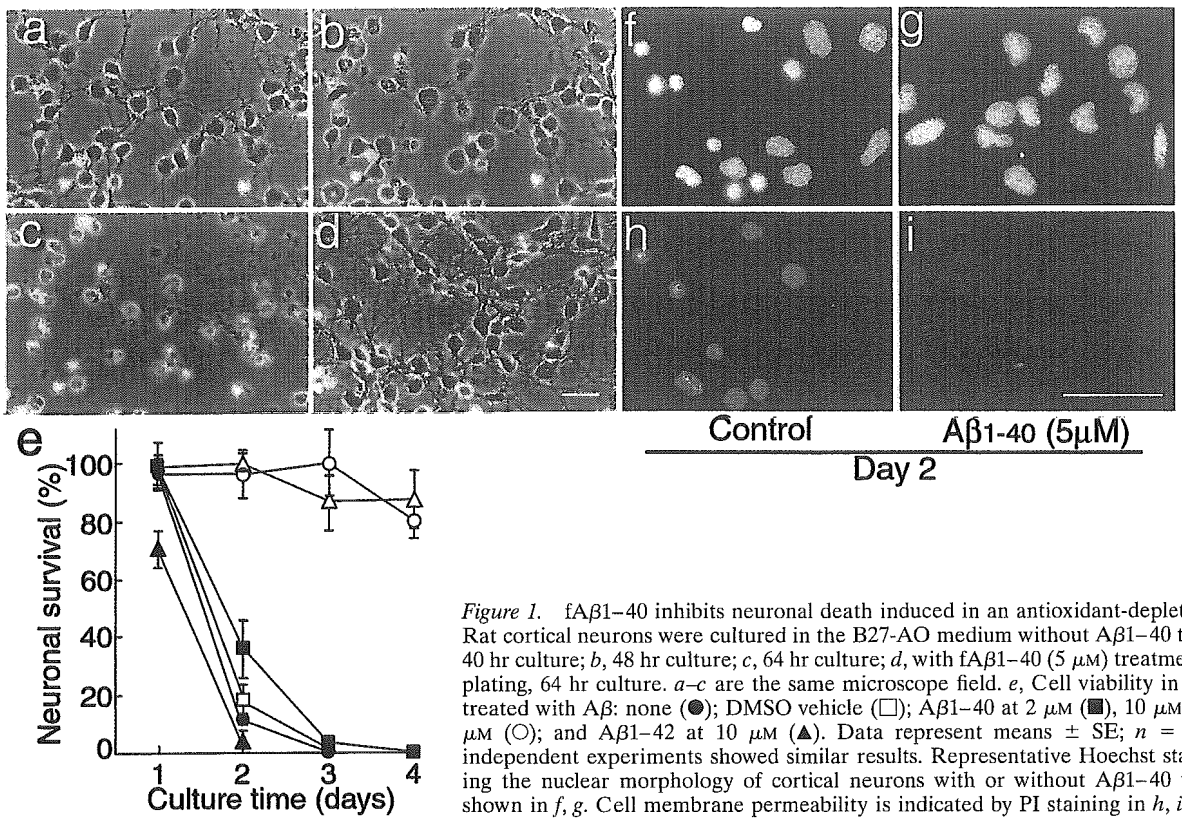

Figure 1. fAβ1–40 inhibits neuronal death induced in an antioxidant-depleted medium. Rat cortical neurons were cultured in the B27-AO medium without Aβ1–40 treatment: *a*, 40 hr culture; *b*, 48 hr culture; *c*, 64 hr culture; *d*, with fAβ1–40 (5 μM) treatment 4 hr after plating, 64 hr culture. *a–c* are the same microscope field. *e*, Cell viability in the cultures treated with Aβ: none (●); DMSO vehicle (□); Aβ1–40 at 2 μM (■), 10 μM (△), and 20 μM (○); and Aβ1–42 at 10 μM (▲). Data represent means ± SE; $n = 6$ each. Six independent experiments showed similar results. Representative Hoechst staining showing the nuclear morphology of cortical neurons with or without Aβ1–40 treatment is shown in *f*, *g*. Cell membrane permeability is indicated by PI staining in *h*, *i*.

nuclei of dead neurons were shrunken as demonstrated by Hoechst 22336 and PI staining (Figs. 1*f*,*h*). The effect of freshly prepared Aβ1–42 on neuronal viability was also examined. fAβ1–42 could not inhibit neurotoxicity but rather promoted neuronal death (Fig. 1*e*).

Monomeric Aβ1–40, but not oligomeric Aβ1–40, has an ability to protect neurons in the B27-AO medium

We examined the effect of incubated Aβ1–40 (iAβ1–40), which was filtered and the protein concentration of which was determined before addition, on neuronal viability cultured in the B27-AO medium. As shown in Figure 2*a*, neuronal death occurred 72 hr after the commencement of the treatment, which was completely inhibited by fAβ1–40, but not by iAβ1–40, at a concentration of 5 μM. Results of the quantitative analysis of neuronal viability within 72 hr of incubation are shown in Figure 1*b*, showing that fAβ1–40 at concentrations of 5 and 10 μM completely inhibited neuronal death, whereas iAβ1–40 inhibited neuronal death at 10 μM but not at 5 μM. To determine the oligomeric state of Aβ, the reaction of the conditioned medium of each culture with thioflavin-T was determined. As shown in Figure 2*c*, the value of the conditioned medium of the cultures treated with iAβ1–40 was significantly higher than that treated with fAβ1–40, indicating that iAβ1–40 contains highly oligomerized Aβ. To determine more directly that the amount of monomeric Aβ was decreased and that of oligomeric Aβ was increased, a cross-linking study of each Aβ sample was performed. As shown in Figure 2*d*, fAβ1–40 contains mostly monomers, whereas iAβ1–40 contains many oligomers, including dimers, trimers, and tetramers, in addition to decreased levels of monomers. These results indicate that Aβ monomers have a neuroprotective activity and that the lack of neuroprotective activity of iAβ1–40 at 5 μM is not caused by its toxic effect on neurons but rather by the low levels of monomers.

Metal-binding protein and metal chelators inhibit neuronal death in the B27-AO medium

Because neurotoxicity was induced in the media deficient of antioxidant reagents, it is reasonable to assume that the Aβ-mediated neuronal protection may possibly be explained by an antioxidant action of Aβ. Antioxidant actions include a direct antioxidant effect, and the indirect actions of fAβ1–40 include quenching of metal ions to inhibit secondary generation of free radicals. Thus, we examined the effect of molecules that have antioxidant activities. As shown in Figure 3*a*, catalase, glutathione, vitamin E acetate, and vitamin E inhibited neuronal death at culture day 2. Catalase and vitamin E acetate and vitamin E partially and completely inhibited cell death at culture day 4, respectively; however, SOD did not show any neuroprotective activity. Because we have observed that the N2 supplements (Bottenstein and Sato, 1979) inhibited neuronal death induced by incubation in the B27-AO medium, we examined the inhibitory effect of each component of N2 supplements. Figure 3*b* shows that among the components examined, only transferrin successfully inhibited neuronal death. Because transferrin is known to bind iron, inhibiting cell death by quenching the iron-dependent generation of reactive oxygen radicals (Halliwell and Gutteridge, 1989), it is reasonable to postulate that iron in DMEM/F12 plays a critical role in neuronal death in the B27-AO medium. Thus, we next examined the effect of various iron chelators on neuronal death under these conditions. EDTA (400 μM), CDTA (40 μM), and DTPA (8 μM) protected neurons against toxicity induced in the B27-AO medium at culture day 4 (Table 1).

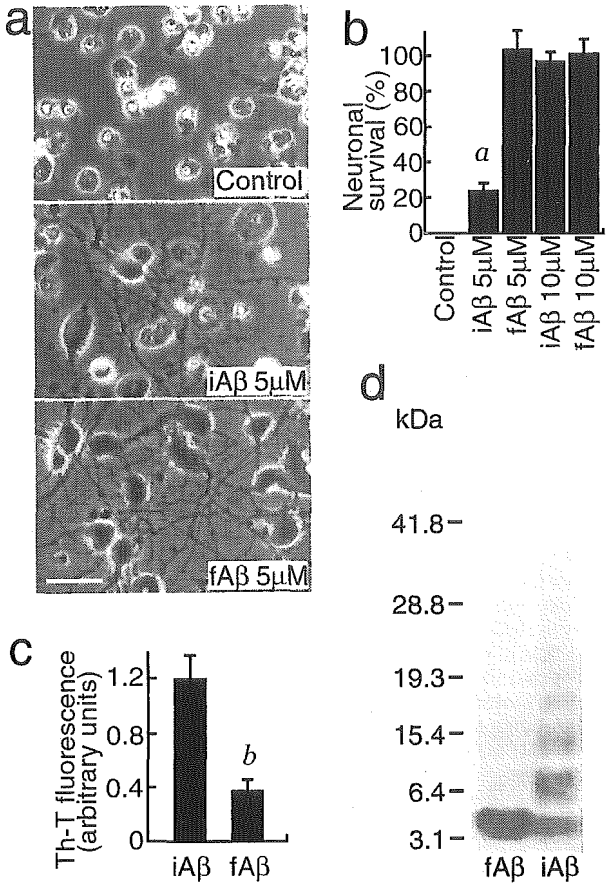

Figure 2. fAβ1–40 but not iAβ1–40 protects neurons in the B27-AO medium. Neurons were treated with fAβ1–40 or iAβ1–40 24 hr after plating. Phase-contrast photomicrographs were taken (*a*), and the cell viability was determined (*b*) 48 hr after the commencement of each treatment. *a*, $p < 0.0001$ versus fAβ1–40 (5 μM), iAβ1–40 (10 μM), and fAβ1–40 (10 μM). *c*, Thioflavin-T fluorescence with the conditioned medium of each cultured neuron treated with fAβ1–40 or iAβ1–40 for 3 d. *b*, $p < 0.01$ versus iAβ1–40. *d*, Detection of oligomeric Aβ in fAβ and iAβ samples by cross-linking with glutaraldehyde. fAβ1–40 or iAβ1–40 (2.5 μg) was cross-linked with glutaraldehyde and subjected to a 4–20% SDS-PAGE. The gel was then visualized by silver staining.

Monomeric Aβ1–40 protects neurons against iron- and copper-mediated neuronal toxicity

Because the culture medium, DMEM/F12 supplemented with B27-AO, contains 1.5 μM Fe (II), 124 nM Fe(III), and 5.2 nM Cu(II), our findings that neuronal death induced in the B27-AO medium is prevented by antioxidant scavengers, metal chelators, and transferrin indicate that neurotoxicity is induced by oxygen radicals generated in an Fe(II)-mediated manner. Thus, we next determined whether transition metal ions, such as iron and copper ions, and H_2O_2 exhibit neurotoxicity on cultured neurons, and whether fAβ1–40 has the ability to prevent this toxicity. Twenty-four hours after plating, neuronal cultures were treated with 1.5 μM $CuSO_4$, 3.0 μM $FeSO_4$, 25 μM $Fe(NO_3)_3$, and 30 μM H_2O_2 in the presence or absence of 5 μM fAβ1–40 in the N2 medium. After 24 hr incubation, photographs were taken, and the neuronal viability was determined. As shown in Figure 4, Cu(II), Fe(II), Fe(III), and H_2O_2 caused cell death (*a*, *c*, *e*, and *g*, respectively). fAβ1–40 at a concentration of 5 μM inhibited cell death caused by these metals (Fig. 4*b*,*d*,*f*) but did not inhibit cell death caused by H_2O_2 (Fig. 4*h*), indicating that protection of neurons by fAβ1–40

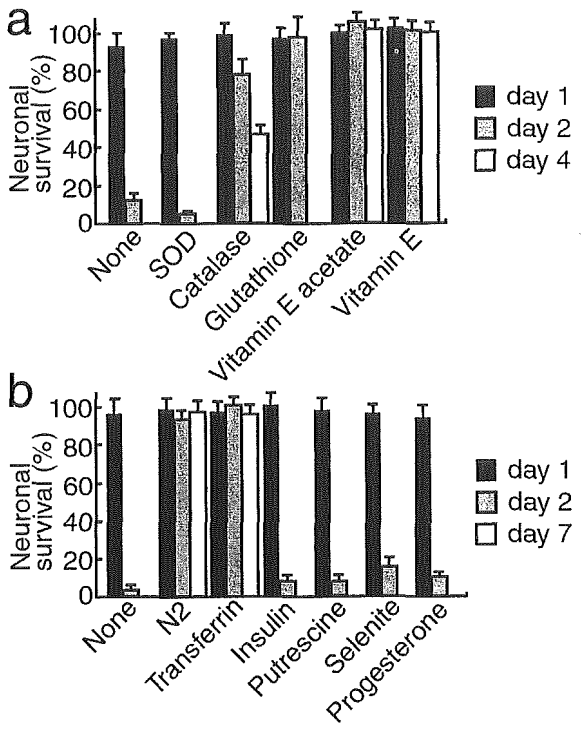

Figure 3. Transferrin and antioxidant scavengers inhibit neuronal death that occurred in the B27-AO medium. *a*, SOD (1500 U/ml), catalase (21,600 U/ml), glutathione (450 μg/ml), vitamin E acetate (1 μg/ml), or vitamin E (1 μg/ml) was added to neuronal cultures maintained in the B27-AO medium 4 hr after plating. *b*, N2 supplements or each component of N2 supplements, transferrin (100 μg/ml), insulin (5 μg/ml), progesterone (0.0063 μg/ml), putrescine (16.11 μg/ml), and selenite (0.0052 μg/ml) was added to neuronal cultures maintained in the B27-AO medium 4 hr after plating. Neuronal viability was determined as described in Materials and Methods at culture days 1, 2, and 4 (*a*) or 1, 2, and 7 (*b*).

Table 1. Metal chelators inhibit neuronal death induced in the B27-AO medium

Chelators	Concentration (μM)	Viability (% of control)
None	0	0
EDTA	400	60 ± 3
CDTA	40	99 ± 4
DTPA	8	93 ± 7

Primary cortical neurons were cultured in the B27-AO medium. Four hours after plating, the cultures were incubated with metal chelators. Cell viability was determined 48 h after the start of treatment. The data represent means ± SE. $n = 6$ each. Three independent experiments showed similar results.

is not caused by a direct antioxidant activity but by an indirect one via interaction with metal ions. The quantitative analysis of these experiments is shown in Figure 4*i*. We performed additional experiments to determine the effect of transferrin on neuronal toxicity induced by these metals. We found that 3.8 μM transferrin inhibited 3.0 μM Fe(II)- and 25 μM Fe(III)-mediated neurotoxicity, but even 13 μM transferrin did not inhibit 1.5 μM Cu(II)-mediated neurotoxicity (data not shown), supporting the idea that Fe(II) but not Cu(II) is responsible for the generation of oxygen radicals and induces toxicity. This is supported by the fact that the B27-AO medium contains 1.5 μM Fe(II), which is sufficiently high to induce cell toxicity, whereas it contains much lower concentrations of Cu(II) and Fe(III).

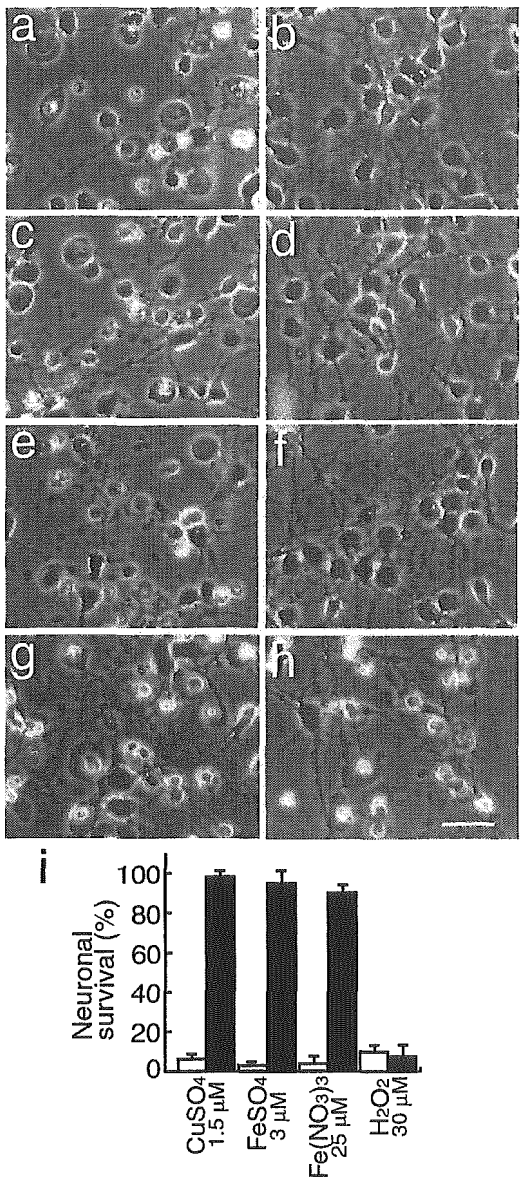

Figure 4. f Aβ1–40 inhibits neuronal death induced by transition-metal ions. Neurons were cultured in N2 medium for 24 hr, followed by treatment with 1.5 μM $CuSO_4$ (*a*, *b*), 3.0 μM Fe SO_4 (*c*, *d*), 25 μM $Fe(NO_3)_3$, (*e*, *f*), and 30 μM H_2O_2 (*g*, *h*), and incubated for another 24 hr; photographs were taken to determine cell viability. *a*, *c*, *e*, and *g* represent control cultures, and *b*, *d*, *f*, and *h* represent neurons treated with fAβ1–40 (5 μM) in addition to metal ions. *i*, Quantitative analysis of these treatments 24 hr after the commencement of the metal treatment. *Open* and *closed bars* indicate cell viability in the cultures in the absence or presence, respectively, of fAβ1–40 (5 μM).

Monomeric Aβ1–40 inhibits vitamin C-mediated reduction of Fe(III)

Because reduced metal ions are known to generate oxygen radicals that initiate subsequent reactions of radical productions (Halliwell and Gutteridge, 1984), we determined whether fAβ1–40 has any effect on Fe(III) reduction. To examine the inhibitory effect of fAβ1–40 on Fe(III) reduction, a vitamin C-mediated metal reduction system was used. As shown in Figure 5*a*, fAβ1–40 inhibited Fe(III) reduction mediated by vitamin C. In addition to fAβ1–40, fAβ1–42, Aβ1–16, Aβ25–35, and a metal ion chelator, DTPA, also inhibited Fe(III) reduction. Because the

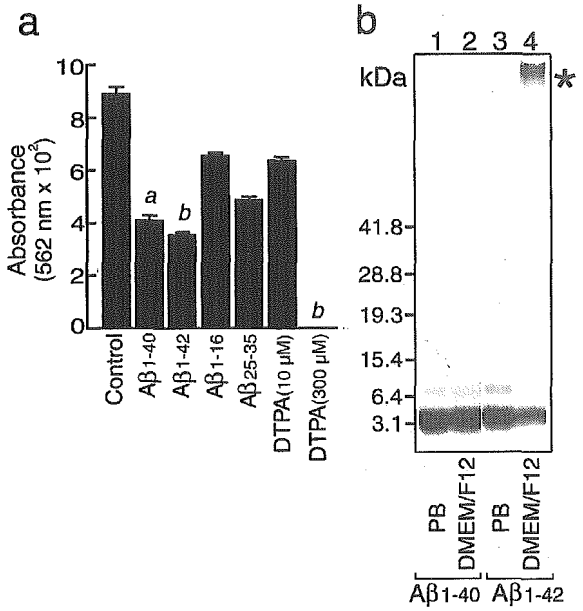

Figure 5. Inhibitory effect of Aβ peptides on vitamin C-mediated Fe(III) reduction and the aggregation state of Aβ peptides in PB and DMEM/F12. *a*, Aβ peptides were incubated with Fe(III) (25 μM) and PDT (250 μM), followed by the addition of vitamin C (10 μM) and subsequent incubation for 14 hr at 37°C. The effects of freshly dissolved Aβ peptides (10 μM) (fAβ1–40, fAβ1–42, fAβ1–16, and fAβ25–35, all of which were dissolved in distilled water to make a stock solution at 200 μM) and DTPA (10 and 300 μM) on the reduction of Fe(III) were determined. The amount of reduced iron ions was determined by measuring the absorbance at 562 nm. Data represent means ± SE; $n = 5$ replicate wells. $p < 0.001$ (*a*) and $p < 0.0001$ (*b*) versus control. *b*, Freshly dissolved Aβ1–40 and Aβ1–42 peptides at 20 μM were incubated for 3 hr at 37°C in 8 mM sodium phosphate buffer, pH 7.4 (*lanes 1*, *3*), or in DMEM/F12 medium (*lanes 2*, *4*). The aggregation state of Aβ1–40 (*lanes 1*, *2*) and Aβ1–42 (*lane 3*, *4*) was visualized by SDS-PAGE and silver staining after cross-linking as described in Materials and Methods. Note that Aβ1–42 aggregated immediately in DMEM/F12 (*), but the majority of both peptides, Aβ1–40 in both solutions and Aβ1–42 in PB, remained as a monomer.

action of Aβ is known to depend on the state of aggregation of the peptides, we next determined the aggregation states of Aβ used in this study by cross-linking of peptides with glutaraldehyde and subsequent silver staining. As shown in Figure 5*b*, most of both Aβ1–40 and Aβ1–42 incubated in 8 mM sodium phosphate buffer and Aβ1–40 incubated in DMEM/F12 for 3 hr were found to be monomers, whereas fAβ1–42 incubated in DMEM/F12 for 3 hr was found to form aggregation (Fig. 5*b*, *), and the amount of monomeric Aβ1–42 was significantly decreased (Fig. 5*b*).

Generation of superoxides in the B27-AO medium and Fe(II)-induced lipid peroxidation are inhibited by monomeric Aβ1–40

Using HE dye, we examined whether the generation of oxygen radicals is enhanced in the B27-AO medium and whether this enhancement is inhibited by fAβ1–40. As shown in Figure 6*a*, strong signals of oxidized ethidium dye were observed in some viable neurons with swollen cell bodies (Fig. 6*a*, *arrows*) and dead neurons with shrunken cell bodies (Fig. 6*c*), whereas the signals with ethidium dye in the cultures treated with fAβ1–40 (5 μM) were not detected (Fig. 6*b*). We then examined the effect of fAβ1–40 on Fe(II)-induced lipid peroxidation in rat brain cortices by investigating the production of 4-HNE-modified proteins, a product of lipid peroxidation in rat brains, using a monoclonal antibody against 4-HNE-modified proteins. As shown in Figure

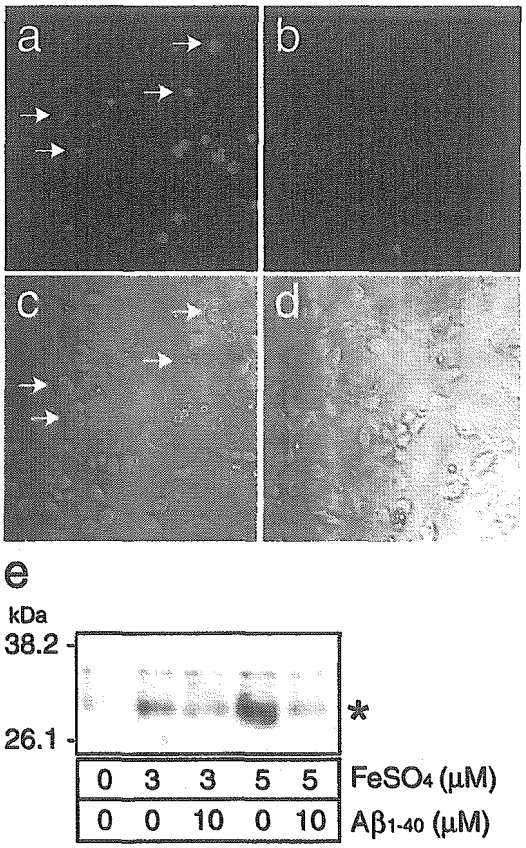

Figure 6. fAβ1–40 inhibits the generation of superoxide and lipid peroxidation. Neurons were treated with (*a*, *c*) or without (*b*, *d*) 5 μM fAβ1–40 4 hr after plating and were cultured for 48 hr in the B27-AO medium. The cultures were then incubated with 5 μM HE fluorescence (*a*, *b*) for 30 min, and transmissive light micrographs of these cultures were taken. Note that the increased signal of superoxides was observed in swollen neurons (*arrows*) as well as in shrunken neurons in cultures without fAβ (*a*). *e*, The effect of Aβ on the production of lipid peroxidation in rat cerebral cortices in the presence of Fe(II). Cerebral cortices were isolated, minced with a cutter, and incubated in PBS in the presence of 3 and 5 μM Fe(II) with or without fAβ1–40 at 10 μM for 4 hr at 37°C. The fragments were then homogenized in RIPA buffer and centrifuged at 10,000 × *g* for 10 min at 4°C. The supernatant of the homogenate was subjected to Western blot analysis using anti-4-HNE antibody as the primary antibody.

6*e* (*), the amount of 4-HNE-modified proteins increased in brains incubated in PBS in the presence of 3 and 5 μM Fe(II), whereas treatment with 10 μM fAβ1–40 attenuated this increase. This result indicates that fAβ1–40 prevented lipid peroxidation of the brain tissues induced by oxygen radicals generated by the Fenton reaction.

Comparison of effects of various kinds of Aβ species on neuronal protection

We examined the neuroprotective effect of Aβ1–42, Aβ1–16, and Aβ25–35, in addition to Aβ1–40, on cultured cells incubated in the B27-AO medium. Treatment of Aβ1–40 at a concentration of 5 μM inhibited neuronal death at a percentage of 95 ± 5, whereas Aβ1–42 at concentrations of 0.01, 0.1, 1, 2, 5, 10, and 20 μM, Aβ1–16 at concentrations of 1, 2, 5, 10, 20, and 40, or Aβ25–35 at concentrations of 1, 2, 5, 10, 20, and 40 did not prevent neuronal death 48 hr after the commencement of incubation (Table 2). In the case of Aβ1–42, the thioflavin-T value of the culture medium at the end of treatment significantly increased compared with that of the culture medium treated with Aβ1–40, Aβ1–16, or Aβ25–35, indicating that Aβ1–42 becomes highly aggregated in a culture medium. However, because Aβ1–40, when it remains as a monomer, has an antioxidant effect in the *in vitro* assay system (Fig. 5*a*), we next performed an experiment to determine whether monomeric Aβ1–42 at a concentration of 5 μM has a neuroprotective effect on neurons. Because Congo red is known to inhibit oligomerization of Aβ by stabilizing Aβ monomer (Podlisny et al., 1995, 1998), we used Congo red to maintain Aβ1–42 as a monomer. As shown in Table 2, concurrent treatment of 100 μM Congo red with 5 μM Aβ1–42 inhibited neuronal death, whereas treatment with 100 μM Congo red alone did not. The thioflavin-T value of these conditioned media was not determined, because Congo red affects the thioflavin-T assay system. These data indicate that monomeric Aβ, regardless of its species, Aβ1–40 or Aβ1–42, rescues neurons.

Effect of tachykinin neuropeptides on monomeric Aβ1–40-mediated neuroprotection

Because a previous study has demonstrated the neurotrophic effects of Aβ1–40, which can be reversed by tachykinin neuropeptides (Yankner et al., 1990), we further examined whether the neuroprotective effect of monomeric Aβ1–40 is inhibited by tachykinin neuropeptides. In our culture system, takykinine neuropeptides such as substance P, physalaemin, eledoisin, neurokinin A, and neurokinin B at 1, 2, 5, 10, and 20 μM did not inhibit neuronal death. Moreover, substance P and physalaemin did not inhibit the neuroprotective effect of Aβ1–40 (Table 3). These results indicate that the mechanism underlying the neurotrophic effects of Aβ1–40 is different from that underlying the antioxidant functions of monomeric Aβ.

DISCUSSION

In this study, we demonstrated a novel function of monomeric Aβ1–40 as an antioxidant molecule on cultured neurons. Monomeric Aβ1–40 exhibits a neuroprotective effect on neurons by quenching transition metal-mediated oxygen radical generation; however, oligomeric Aβ1–40 loses its neuroprotective activity. Monomeric Aβ1–42 also exhibits a neuroprotective effect; however, when monomeric Aβ1–42 is incubated in the culture medium, it rapidly aggregates and exhibits neurotoxicity, whereas monomeric Aβ1–40 remains as a monomer under the same conditions and protects neurons. These findings indicate a novel concept that the biological action of Aβ is dualistic. Aβ, as a monomer, functions as an antioxidant molecule, preventing the generation of oxygen radicals, whereas oligomerized or aggregated Aβ not only loses its antioxidant activity but also contributes to the generation of oxygen radicals (Kay, 1997; Monji et al., 2001a,b), disrupts lipid homeostasis (Michikawa et al., 2001; Gong et al., 2002), and eventually exhibits neurotoxicity (Mattson et al., 1993; Pike et al., 1993; Lorenzo and Yankner, 1994).

Neuronal death induced in the B27-AO medium is inhibited by the addition of radical scavengers, indicating that neuronal toxicity is caused by oxygen radicals. The B27-AO medium contains 1.5 μM Fe(II), 124 nM Fe(III), and 5.2 nM Cu(II), and redox-active transition metals such as iron and copper are known to stimulate oxygen radical chain reactions (Halliwell and Gutteridge, 1984). Because 1.5 μM or higher concentrations of Fe(II) and Cu(II) induce neuronal death in culture [our unpublished data and previous reports (White et al., 1999; Wang and Cynader, 2001)], Fe(II) is most likely responsible for inducing neurotoxicity by generating oxygen radicals in the B27-AO medium. Furthermore,

Table 2. Effect of various kinds of Aβ peptides on neuronal viability in the B27-AO medium

Peptides	Concentration Aβ (μM)	Viability (% of control)	Thioflavin-T arbitrary unit (Aβ, 5 μM)
None	0	0	0
Aβ1–40	5	95 ± 5	0.11 ± 0.12
Aβ1–42	0.01, 0.1, 1, 2, 5, 10, 20	0	0.51 ± 0.12*
Aβ1–16	1, 2, 5, 10, 20, 40	0	0.02 ± 0.01
Aβ25–35	1, 2, 5, 10, 20, 40	0	0.02 ± 0.04
Aβ40-1	1, 2, 5, 10, 20, 40	0	ND
Aβ1–42 + CR (100 μM)	5	96 ± 4	ND
CR (100 μM)	0	0	ND

Primary cortical neurons were cultured in the B27-AO medium. Four hours after plating the cultures were incubated with various kinds of Aβ peptides. In the case of Congo red (CR) treatment, the cultures were incubated with CR (100 μM), with or without Aβ1–42 (5 μM). Cell viability was determined 48 hr after the start of treatment. The data represent means ± SE. $n = 6$ each. Three independent experiments showed similar results. *$p < 0.0001$ versus Aβ1–40, Aβ1–16, and Aβ25–35. ND, Not determined.

Table 3. Effect of substance P and physalaemin on the neuroprotective effect of monomeric Aβ1–40 in the B27-AO medium

Treatment	Viability (% of control)
None	0
Aβ1–40 (10 μM)	95 ± 5
Aβ1–40 (10 μM) + substance P (20 μM)	101 ± 12
Aβ1–40 (10 μM) + physalaemin (20 μM)	94 ± 6
Substance P (1, 2, 5, 10, 20 μM)	0
Physalaemin (1, 2, 5, 10, 20 μM)	0
Eledoisin (1, 2, 5, 10, 20 μM)	0
Neurokinin A (1, 2, 5, 10, 20 μM)	0
Neurokinin B (1, 2, 5, 10, 20 μM)	0

Primary cortical neurons were cultured in the B27-AO medium. Four hours after plating the cultures were incubated with 10 μM freshly dissolved Aβ1–40 in the presence or absence of substance P (20 μM) or physalaemin (20 μM). The cultures were also treated with substance P, physalaemin, eledoisin, neurokinin A, and neurokinin B at various concentrations. Cell viability was determined 48 hr after the start of treatment. The data represent means ± SE. $n = 6$ each.

the facts that transferrin successively protects neurons in the B27-AO medium (Fig. 3*b*) and inhibits Fe(II)-mediated neuronal death in N2 medium, whereas it does not prevent Cu(II)-induced neuronal death (data not shown), strongly support this notion. Thus, it is possible that fAβ1–40 protects neurons from oxygen radicals generated in an Fe(II)-mediated manner.

Antioxidant actions include a direct antioxidant action such as that of scavengers and indirect actions including the quenching metal ions to inhibit secondary generation of free radicals. The neuroprotective activity of monomeric Aβ1–40 includes an inhibitory effect on the generation of superoxides in cultured neurons and lipid peroxidation in brains (Fig. 6). Furthermore, the direct inhibitory effects of monomeric Aβ1–40 on metal reduction induced by vitamin C are also demonstrated (Fig. 5). These findings, together with the result showing that monomeric Aβ1–40 does not serve as a radical scavenger (Fig. 4), indicate that the neuroprotective activity of Aβ1–40 is not caused by a direct antioxidant effect but rather by an indirect effect of this peptide, probably the sequestration of metal ions leading to the quenching of the secondary generation of oxygen radicals as other metal-binding proteins do (Halliwell and Gutteridge, 1989).

Free-radical involvement in AD pathogenesis is a well established hypothesis (Lovell et al., 1998a; Markesbery and Lovell, 1998). Aβ is widely believed to serve as a neurotoxic molecule by producing oxygen radicals leading to cell dysfunction and death (Behl et al., 1994; Hensley et al., 1994). The oxygen radicals generated by the interaction of Aβ with redox-active metal ions are suggested to be the possible source of Aβ neurotoxicity, which is suppressed by the redox-inactive form of zinc or metal ion chelators (Huang et al., 1999a,b; Cuajungco et al., 2000a). These lines of evidence seem to contradict our present results that monomeric Aβ1–40 is a potent antioxidant molecule. This discrepancy can be explained by the notion that the action of Aβ is aggregation state-dependent. We show that monomeric Aβ1–40 protects neurons from metal-induced neurotoxicity, whereas iAβ1–40 contains fewer Aβ monomers but more oligomers (Fig. 2*d*), which could be the reason for the loss of its neuroprotective ability. This is also the case for Aβ1–42, because we have found that Aβ1–42, remaining as a monomer in PB, inhibits the reduction of Fe(III) caused by vitamin C as does Aβ1–40 (Fig. 5*a*), indicating that monomeric Aβ1–42 also functions as an antioxidant molecule. In addition, the finding that Aβ1–42, when it is maintained as a monomer by coincubation with Congo red in DMEM/F12 medium, exhibits neuroprotective activity (Table 2) strongly supports this notion. However, when fAβ1–42 is incubated in DMEM/F12 medium that contains salt, it aggregates rapidly (Fig. 5*b*, Table 2) and exhibits neurotoxicity (Fig. 1*e*, Table 2), whereas fAβ1–40 remaining as a monomer under the same conditions protects neurons (Figs. 1*e*, 5*b*). Thus, under physiological conditions, Aβ1–42, a highly amyloidogenic peptide, rapidly aggregates, loses its neuroprotective activity, generates free radicals, and subsequently exhibits neurotoxicity (Pike et al., 1993; Lorenzo and Yankner, 1994; Roher et al., 1996; Kay, 1997; Huang et al., 1999b; Cuajungco et al., 2000b; Monji et al., 2001a,b). These lines of evidence suggest that it may not the differences in Aβ species, Aβ1–40 or Aβ1–42, but those in the state of aggregation, monomers, or other states of aggregation such as oligomers or fibrils, that determine whether the action of Aβ is either neuroprotective or neurotoxic.

Another possible explanation for the discrepancy between the effect of Aβ1–40 and that of Aβ1–42 on neuronal survival may be that at low iron/Aβ binding ratios, iron is captured by Aβ and sequestered from inducing oxygen radical generation, but at higher iron/Aβ ratios, the interaction of Aβ and iron promotes oxygen radical generation (Huang et al., 1999a). Because Aβ1–42 is suggested to bind iron with greater affinity than Aβ1–40 (Atwood et al., 2000), it may be possible to postulate that Aβ1–42 may acquire gain of adverse action at lower concentrations than Aβ1–40.

One may say that because a previous study has demonstrated that aggregated Aβ does not lose the stoichiometry of copper binding (Atwood et al., 2000), an increased amount of oligomer-

ized Aβ may undergo oxidization, reduce metal ions, and serve as an oxygen radical generator (Huang et al., 1999a), leading to neuronal death. Actually, at present we have no evidence indicating that oligomeric Aβ has lesser binding affinity to iron than monomeric Aβ. This may be the case for Aβ1–42, because Aβ1–42 that rapidly aggregates in the culture medium not only loses its neuroprotective activity but also exhibits neurotoxicity (Fig. 1*e*); however, this may not be the case for Aβ1–40. Our findings that 5 μM iAβ1–40 loses its neuroprotective effect on neurons, whereas 10 μM iAβ1–40 protects neurons (Fig. 2*b*), do not favor the idea that the loss of neuroprotective function is caused by oxidized oligomeric Aβ but favor the notion that monomeric but not oligomeric Aβ1–40 can serve as an antioxidant molecule.

The last question to be addressed is that the neuroprotective effects of monomeric Aβ1–40 shown in our present study are the same as the previously reported neurotrophic effects of Aβ1–40, which can be reversed by tachykinin neuropeptides (Yankner et al., 1990). However, monomeric Aβ1–40 has a neuroprotective effect even on mature neurons at high concentrations, whereas takykinin neuropeptides including substance P and physalaemin at 10 and 20 μM did not inhibit neuronal death in our culture system. Moreover, substance P and physalaemin did not reverse the neuroprotective effect of Aβ1–40 (Table 3), indicating that the mechanism underlying the neurotrophic effects of Aβ1–40 is different from that underlying the antioxidant functions of monomeric Aβ.

The notion that monomeric Aβ1–40 functions as an antioxidant is supported by previous studies showing that the surrounding regions of Aβ deposits in the brains of patients with AD and Down's syndrome have no damage (Nunomura et al., 2000, 2001) and that the inverse correlation is found between Aβ burden and levels of oxidized nucleic acids in AD brain (Cuajungco et al., 2000b). Interestingly, a recent report suggests that brain oxidative damage occurs before Aβ accumulation in the brains of a model mouse of AD amyloidosis (Pratico et al., 2001). Previous reports have shown that Aβ1–42 accumulates with aging, whereas Aβ1–40 does not but accumulates in AD brains (Funato et al., 1998), and that oxidative stress promotes amyloidogenesis (Misonou et al., 2000). These lines of evidence may allow us to assume that oxygen radicals generated in an age-dependent manner enhance generation of Aβ, which may protect neurons from oxygen radical toxicity generated by metal-dependent chain reactions. However, with the increasing amount of Aβ serving as an antioxidant, Aβ aggregates with longer incubation periods in extracellular local fluid and, in turn, exhibits neurotoxicity.

On the basis of our findings, we envisage that Aβ may serve dual actions both by being involved in mechanisms attempting to quench oxidative stress and neurotoxicity probably by sequestrating metal ions when Aβ is in a monomeric state and by exhibiting neurotoxicity when Aβ is highly oligomerized and aggregated by generating oxygen radicals in a metal-mediated manner. Hence, although the toxic actions of Aβ have been exaggerated to date, our observations may provide a new insight into the strategies for development of AD therapy that not only reduction of the amount of Aβ but also inhibition of Aβ aggregation could be the pivotal target for AD therapy.

REFERENCES

Atwood CS, Moir RD, Huang X, Scarpa RC, Bacarra NM, Romano DM, Hartshorn MA, Tanzi RE, Bush AI (1998) Dramatic aggregation of Alzheimer Aβ by Cu(II) is induced by conditions representing physiological acidosis. J Biol Chem 273:12817–12826.

Atwood CS, Scarpa RC, Huang X, Moir RD, Jones WD, Fairlie DP, Tanzi RE, Bush AI (2000) Characterization of copper interactions with alzheimer amyloid β peptides: identification of an attomolar-affinity copper binding site on amyloid β1–42. J Neurochem 75:1219–1233.

Behl C, Davis JB, Lesley R, Schubert D (1994) Hydrogen peroxide mediates amyloid β-protein toxicity. Cell 77:817–827.

Bindokas VP, Jordan J, Lee CC, Miller RJ (1996) Superoxide production in rat hippocampal neurons: selective imaging with hydroethidine. J Neurosci 16:1324–1336.

Bottenstein JE, Sato GH (1979) Growth of a rat neuroblastoma cell line in serum-free supplemented medium. Proc Natl Acad Sci USA 76:514–517.

Bush AI, Pettingell Jr WH, Paradis MD, Tanzi RE (1994a) Modulation of Aβ adhesiveness and secretase site cleavage by zinc. J Biol Chem 269:12152–12158.

Bush AI, Pettingell WH, Multhaup G, Paradis MD, Vonsattel JP, Gusella JF, Beyreuther K, Masters CL, Tanzi RE (1994b) Rapid induction of Alzheimer Aβ amyloid formation by zinc. Science 265:1464–1467.

Cherny RA, Atwood CS, Xilinas ME, Gray DN, Jones WD, McLean CA, Barnham KJ, Volitakis I, Fraser FW, Kim Y, Huang X, Goldstein LE, Moir RD, Lim JT, Beyreuther K, Zheng H, Tanzi RE, Masters CL, Bush AI (2001) Treatment with a copper-zinc chelator markedly and rapidly inhibits β-amyloid accumulation in Alzheimer's disease transgenic mice. Neuron 30:665–676.

Cuajungco MP, Faget KY, Huang X, Tanzi RE, Bush AI (2000a) Metal chelation as a potential therapy for Alzheimer's disease. Ann NY Acad Sci 920:292–304.

Cuajungco MP, Goldstein LE, Nunomura A, Smith MA, Lim JT, Atwood CS, Huang X, Farrag YW, Perry G, Bush AI (2000b) Evidence that the β-amyloid plaques of Alzheimer's disease represent the redox-silencing and entombment of Aβ by zinc. J Biol Chem 275: 19439–19442.

Funato H, Yoshimura M, Kusui K, Tamaoka A, Ishikawa K, Ohkoshi N, Namekata K, Okeda R, Ihara Y (1998) Quantitation of amyloid β-protein (Aβ) in the cortex during aging and in Alzheimer's disease. Am J Pathol 152:1633–1640.

Glenner GG, Wong CW (1984) Alzheimer's disease: initial report of the purification and characterization of a novel cerebrovascular amyloid protein. Biochem Biophys Res Commun 120:885–890.

Gong JS, Sawamura N, Zou K, Sakai J, Yanagisawa K, Michikawa M (2002) Amyloid β-protein affects cholesterol metabolism in cultured neurons: implications for pivotal role of cholesterol in the amyloid cascade. J Neurosci Res, in press.

Halliwell B, Gutteridge JM (1984) Oxygen toxicity, oxygen radicals, transition metals and disease. Biochem J 219:1–14.

Halliwell B, Gutteridge JMC (1989) Protection by sequestration of metal ions. In: Free radicals in biology and medicine, Ed 2, pp 131–133. New York: Oxford UP.

Hartley DM, Walsh DM, Ye CP, Diehl T, Vasquez S, Vassilev PM, Teplow DB, Selkoe DJ (1999) Protofibrillar intermediates of amyloid β-protein induce acute electrophysiological changes and progressive neurotoxicity in cortical neurons. J Neurosci 19:8876–8884.

Hensley K, Carney JM, Mattson MP, Aksenova M, Harris M, Wu JF, Floyd RA, Butterfield DA (1994) A model for β-amyloid aggregation and neurotoxicity based on free radical generation by the peptide: relevance to Alzheimer disease. Proc Natl Acad Sci USA 91: 3270–3274.

Huang X, Atwood CS, Moir RD, Hartshorn MA, Vonsattel JP, Tanzi RE, Bush AI (1997) Zinc-induced Alzheimer's Aβ1–40 aggregation is mediated by conformational factors. J Biol Chem 272:26464–26470.

Huang X, Atwood CS, Hartshorn MA, Multhaup G, Goldstein LE, Scarpa RC, Cuajungco MP, Gray DN, Lim J, Moir RD, Tanzi RE, Bush AI (1999a) The Aβ peptide of Alzheimer's disease directly produces hydrogen peroxide through metal ion reduction. Biochemistry 38:7609–7616.

Huang X, Cuajungco MP, Atwood CS, Hartshorn MA, Tyndall JD, Hanson GR, Stokes KC, Leopold M, Multhaup G, Goldstein LE, Scarpa RC, Saunders AJ, Lim J, Moir RD, Glabe C, Bowden EF, Masters CL, Fairlie DP, Tanzi RE, Bush AI (1999b) Cu(II) potentiation of Alzheimer Aβ neurotoxicity. Correlation with cell-free hydrogen peroxide production and metal reduction. J Biol Chem 274:37111–37116.

Ida N, Hartmann T, Pantel J, Schroder J, Zerfass R, Forstl H, Sandbrink R, Masters CL, Beyreuther K (1996) Analysis of heterogeneous A4 peptides in human cerebrospinal fluid and blood by a newly developed sensitive Western blot assay. J Biol Chem 271:22908–22914.

Iwatsubo T, Odaka A, Suzuki N, Mizusawa H, Nukina N, Ihara Y (1994) Visualization of Aβ42(43) and Aβ40 in senile plaques with end-specific Aβ monoclonals: evidence that an initially deposited species is Aβ42(43). Neuron 13:45–53.

Kay CJ (1997) Mechanochemical mechanism for peptidyl free radical generation by amyloid fibrils. FEBS Lett 403:230–235.

Kontush A, Berndt C, Weber W, Akopyan V, Arlt S, Schippling S,

Beisiegel U (2001) Amyloid-β is an antioxidant for lipoproteins in cerebrospinal fluid and plasma. Free Radic Biol Med 30:119–128.
LeVine 3rd H (1995) Soluble multimeric Alzheimer β(1–40) pre-amyloid complexes in dilute solution. Neurobiol Aging 16:755–764.
LeVine 3rd H (1999) Quantification of β-sheet amyloid fibril structures with thioflavin T. Methods Enzymol 309:274–284.
Lorenzo A, Yankner BA (1994) β-amyloid neurotoxicity requires fibril formation and is inhibited by Congo red. Proc Natl Acad Sci USA 91:12243–12247.
Lovell MA, Xie C, Markesbery WR (1998a) Decreased glutathione transferase activity in brain and ventricular fluid in Alzheimer's disease. Neurology 51:1562–1566.
Lovell MA, Robertson JD, Teesdale WJ, Campbell JL, Markesbery WR (1998b) Copper, iron and zinc in Alzheimer's disease senile plaques. J Neurol Sci 158:47–52.
Markesbery WR, Lovell MA (1998) Four-hydroxynonenal, a product of lipid peroxidation, is increased in the brain in Alzheimer's disease. Neurobiol Aging 19:33–36.
Masters CL, Simms G, Weinman NA, Multhaup G, McDonald BL, Beyreuther K (1985) Amyloid plaque core protein in Alzheimer disease and Down syndrome. Proc Natl Acad Sci USA 82:4245–4249.
Mattson MP, Tomaselli KJ, Rydel RE (1993) Calcium-destabilizing and neurodegenerative effects of aggregated β-amyloid peptide are attenuated by basic FGF. Brain Res 621:35–49.
Michikawa M, Yanagisawa K (1998) Apolipoprotein E4 induces neuronal cell death under conditions of suppressed de novo cholesterol synthesis. J Neurosci Res 54:58–67.
Michikawa M, Gong JS, Fan QW, Sawamura N, Yanagisawa K (2001) A novel action of Alzheimer's β-protein (Aβ): oligomeric Aβ promotes lipid release. J Neurosci 21:7226–7235.
Misonou H, Morishima-Kawashima M, Ihara Y (2000) Oxidative stress induces intracellular accumulation of amyloid β-protein (Aβ) in human neuroblastoma cells. Biochemistry 39:6951–6959.
Monji A, Utsumi H, Yoshida I, Hashioka S, Tashiro K, Tashiro N (2001a) The relationship between Aβ-associated free radical generation and Aβ fibril formation revealed by negative stain electron microscopy and thioflavin-T fluorometric assay. Neurosci Lett 304:65–68.
Monji A, Utsumi H, Ueda T, Imoto T, Yoshida I, Hashioka S, Tashiro K, Tashiro N (2001b) The relationship between the aggregational state of the amyloid-β peptides and free radical generation by the peptides. J Neurochem 77:1425–1432.
Naiki H, Hasegawa K, Yamaguchi I, Nakamura H, Gejyo F, Nakakuki K (1998) Apolipoprotein E and antioxidants have different mechanisms of inhibiting Alzheimer's β-amyloid fibril formation in vitro. Biochemistry 37:17882–17889.
Nunomura A, Perry G, Pappolla MA, Friedland RP, Hirai K, Chiba S, Smith MA (2000) Neuronal oxidative stress precedes amyloid-β deposition in Down syndrome. J Neuropathol Exp Neurol 59:1011–1017.
Nunomura A, Perry G, Aliev G, Hirai K, Takeda A, Balraj EK, Jones PK, Ghanbari H, Wataya T, Shimohama S, Chiba S, Atwood CS, Petersen RB, Smith MA (2001) Oxidative damage is the earliest event in Alzheimer disease. J Neuropathol Exp Neurol 60:759–767.
Pike CJ, Burdick D, Walencewicz AJ, Glabe CG, Cotman CW (1993) Neurodegeneration induced by β-amyloid peptides in vitro: the role of peptide assembly state. J Neurosci 13:1676–1687.
Podlisny MB, Ostaszewski BL, Squazzo SL, Koo EH, Rydell RE, Teplow DB, Selkoe DJ (1995) Aggregation of secreted amyloid β-protein into sodium dodecyl sulfate-stable oligomers in cell culture. J Biol Chem 270:9564–9570.
Podlisny MB, Walsh DM, Amarante P, Ostaszewski BL, Stimson ER, Maggio JE, Teplow DB, Selkoe DJ (1998) Oligomerization of endogenous and synthetic amyloid β-protein at nanomolar levels in cell culture and stabilization of monomer by Congo red. Biochemistry 37:3602–3611.
Pratico D, Uryu K, Leight S, Trojanoswki JQ, Lee VM (2001) Increased lipid peroxidation precedes amyloid plaque formation in an animal model of Alzheimer amyloidosis. J Neurosci 21:4183–4187.
Roher AE, Lowenson JD, Clarke S, Woods AS, Cotter RJ, Gowing E, Ball MJ (1993) β-Amyloid-(1–42) is a major component of cerebrovascular amyloid deposits: implications for the pathology of Alzheimer disease. Proc Natl Acad Sci USA 90:10836–10840.
Roher AE, Chaney MO, Kuo YM, Webster SD, Stine WB, Haverkamp LJ, Woods AS, Cotter RJ, Tuohy JM, Krafft GA, Bonnell BS, Emmerling MR (1996) Morphology and toxicity of Aβ-(1–42) dimer derived from neuritic and vascular amyloid deposits of Alzheimer's disease. J Biol Chem 271:20631–20635.
Sayre LM, Perry G, Harris PL, Liu Y, Schubert KA, Smith MA (2000) In situ oxidative catalysis by neurofibrillary tangles and senile plaques in Alzheimer's disease: a central role for bound transition metals. J Neurochem 74:270–279.
Schubert D, Chevion M (1995) The role of iron in β-amyloid toxicity. Biochem Biophys Res Commun 216:702–707.
Selkoe DJ (1994) Alzheimer's disease: a central role for amyloid. J Neuropathol Exp Neurol 53:438–447.
Smith MA, Harris PL, Sayre LM, Perry G (1997) Iron accumulation in Alzheimer disease is a source of redox-generated free radicals. Proc Natl Acad Sci USA 94:9866–9868.
Vigo-Pelfrey C, Lee D, Keim P, Lieberburg I, Schenk DB (1993) Characterization of β-amyloid peptide from human cerebrospinal fluid. J Neurochem 61:1965–1968.
Wang XF, Cynader MS (2001) Pyruvate released by astrocytes protects neurons from copper-catalyzed cysteine neurotoxicity. J Neurosci 21:3322–3331.
White AR, Multhaup G, Maher F, Bellingham S, Camakaris J, Zheng H, Bush AI, Beyreuther K, Masters CL, Cappai R (1999) The Alzheimer's disease amyloid precursor protein modulates copper-induced toxicity and oxidative stress in primary neuronal cultures. J Neurosci 19:9170–9179.
Yankner BA, Duffy LK, Kirschner DA (1990) Neurotrophic and neurotoxic effects of amyloid β protein: reversal by tachykinin neuropeptides. Science 250:279–282.
Yoshiike Y, Tanemura K, Murayama O, Akagi T, Murayama M, Sato S, Sun X, Tanaka N, Takashima A (2001) New insights on how metals disrupt amyloid β-aggregation and their effects on amyloid-β cytotoxicity. J Biol Chem 276:32293–32299.

INFECTION AND IMMUNITY, Sept. 2002, p. 4818–4825 Vol. 70, No. 9
0019-9567/02/$04.00+0 DOI: 10.1128/IAI.70.9.4818–4825.2002

Macrophage Plasma Membrane Cholesterol Contributes to *Brucella abortus* Infection of Mice

Masahisa Watarai,[1]* Sou-ichi Makino,[1] Makoto Michikawa,[2] Katsuhiko Yanagisawa,[2] Shigeru Murakami,[3] and Toshikazu Shirahata[1]

Department of Veterinary Microbiology, Obihiro University of Agriculture and Veterinary Medicine, Obihiro, Hokkaido 080-8555,[1] Department of Dementia Research, National Institute for Longevity Sciences, Obu, Aichi 474-8522,[2] and Medicinal Research Laboratories, Taisho Pharmaceutical Co., Saitama, Saitama 330-8530,[3] Japan

Received 28 March 2002/Returned for modification 7 May 2002/Accepted 24 May 2002

***Brucella abortus* is a facultative intracellular bacterium capable of surviving inside macrophages. Intracellular replication of *B. abortus* requires the VirB complex, which is highly similar to conjugative DNA transfer systems. In this study, we show that plasma membrane cholesterol of macrophages is required for the VirB-dependent internalization of *B. abortus* and also contributes to the establishment of bacterial infection in mice. The internalization of *B. abortus* was accelerated by treating macrophages with acetylated low-density lipoprotein (acLDL). Treatment of acyl coenzyme A:cholesterol acyltransferase inhibitor, HL-004, to macrophages preloaded with acLDL accelerated the internalization of *B. abortus*. Ketoconazole, which inhibits cholesterol transport from lysosomes to the cell surface, inhibited the internalization and intracellular replication of *B. abortus* in macrophages. The Niemann-Pick C1 gene (NPC1), the gene for Niemann-Pick type C disease, characterized by an accumulation of cholesterol in most tissues, promoted *B. abortus* infection. NPC1-deficient mice were resistant to the bacterial infection. Molecules associated with cholesterol-rich microdomains, "lipid rafts," accumulate in intracellular vesicles of macrophages isolated from NPC1-deficient mice, and the macrophages yielded no intracellular replication of *B. abortus*. Thus, trafficking of cholesterol-associated microdomains controlled by NPC1 is critical for the establishment of *B. abortus* infection.**

Brucella species are facultative intracellular pathogens that survive in a variety of cells, including macrophages, and their virulence and chronic infections are thought to be due to their ability to avoid the killing mechanisms within macrophages (1). The molecular mechanisms of their virulence and chronic infections are incompletely understood. Recent studies with HeLa cells have confirmed these observations, showing that *Brucella* inhibits phagosome-lysosome fusion and transits through an intracellular compartment that resembles autophagosomes. Bacteria replicate in a different compartment, containing protein markers normally associated with the endoplasmic reticulum, as shown by confocal microscopy and immunogold electron microscopy (5, 24). *Brucella* internalizes into macrophages by swimming on the cell surface, with generalized membrane ruffling for several minutes, after which the bacteria are enclosed by macropinosomes (33). "Lipid raft"-associated molecules, such as glycosylphosphatidylinositol (GPI)-anchored proteins, GM1 gangliosides, and cholesterol, have been selectively incorporated into macropinosomes containing *Brucella abortus*. The disruption of lipid rafts on macrophages markedly inhibits the VirB-dependent macropinocytosis and intracellular replication (33). These results indicated that replicative phagosome formation of *B. abortus* is modulated by lipid raft microdomains.

The operon coding for export mechanisms specializing in transferring a variety of multimolecular complexes across the bacterial membrane to the extracellular space or into other cells has been described previously (27). These complexes, named type IV secretion systems, are in *B. abortus* (*virB* genes) (27). This operon comprises 13 open reading frames that share a homology with other bacterial type IV secretion systems involved in the intracellular trafficking of pathogens. Type IV secretion systems export four types of substrates: (i) DNA conjugation intermediates; (ii) the multisubunit pertussis toxin; (iii) monomeric proteins, including primase, RecA, and the *Agrobacterium tumefaciens* VirE2 and VirF proteins; (iv) and the *Helicobacter pylori* CagA protein (4). The RalF protein has been identified as a substrate of the type IV secretion system of *Legionella pneumophila* (20). However, substrates of the VirB secretion system of *B. abortus* and the target of the secretion system in host cells is still unclear.

In this study, we investigated the roles of plasma membrane cholesterol in internalization by the VirB system and the establishment of *B. abortus* infection in mice. Plasma membrane cholesterol associates with lipid raft microdomains. Lipid raft microdomains were originally reported by Simons and van Meer to explain sphingolipid-based sorting properties in cellular membranes (28) and were later proposed to explain cholesterol-based microheterogeneities in the membrane. Plasma membrane cholesterol and intracellular cholesterol trafficking was therefore expected to contribute to internalization and intracellular replication of *B. abortus* in macrophages, because recent evidence indicates that cholesterol sequestration from macrophages inhibits the internalization and intracellular replication of *B. abortus* (21, 33). Our results show that the plasma membrane cholesterol not only influences the bacterial inter-

* Corresponding author. Mailing address: Department of Veterinary Microbiology, Obihiro University of Agriculture and Veterinary Medicine Inada-cho, Obihiro-shi, Hokkaido 080-8555, Japan. Phone: 81-155-49-5387. Fax: 81-155-49-5386. E-mail: watarai@obihiro.ac.jp.

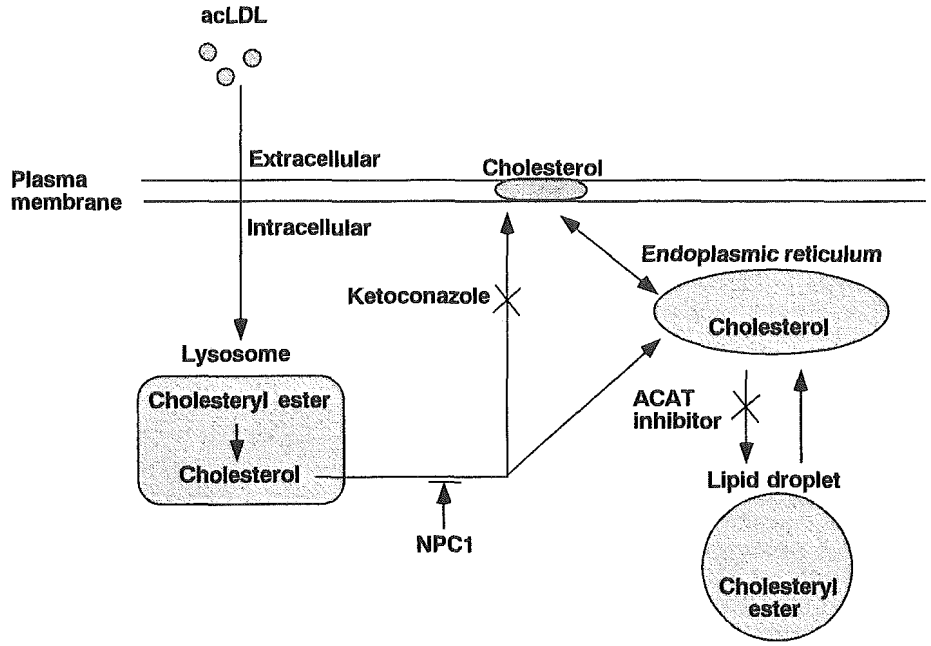

FIG. 1. Schema of cholesterol trafficking in macrophages. The effect of each pharmacological and genetic treatment examined in this study is shown.

nalization and intracellular replication, but also contributes to the establishment of *B. abortus* infection.

MATERIALS AND METHODS

Bacterial strains and mice. All *B. abortus* derivatives were from 544 (ATCC 23448) smooth virulent *B. abortus* biovar 1 strains. Ba598 (544 Δ*virB4*) has been described previously (32). Plasmid pMAW114, which encodes green fluorescence protein (GFP), was constructed by cloning the *Bam*HI-*Bgl*II fragment from the pQBI63 (GFP expression vector; TAKARA, Tokyo, Japan) into *Bam*HI- and *Bgl*II-cleaved pBBR1MCS-2. pMAW114 (GFP^+) was introduced into 544 (wild type) and Ba598 (Δ*virB4*), and the derivatives were designated Ba600 (wild-type GFP^+) and Ba604 (Δ*virB4* GFP^+), respectively (33).

BALB/c mice carrying the genetic mutation for NPC1 were obtained from The Jackson Laboratory (Bar Harbor, Maine) (25).

Cell culture. Bone marrow-derived macrophages from female BALB/c mice were prepared as described previously (32). The macrophages were seeded (2×10^5 to 3×10^5 in each well) in 24-well tissue culture plates for all assays. Macrophages were preloaded with or without acetylated low-density lipoprotein (acLDL) (50 μg/ml) and were treated with or without ketoconazole (10 mg/ml) or acyl coenzyme A:cholesterol acyltransferase (ACAT) inhibitor HL-004 (4 μg/ml; Taisho Pharmaceutical Co.) for 24 h (19).

Detection of intracellular bacteria by fluorescence microscopy. *B. abortus* strains were grown to an A_{600} of 3.2 in brucella broth and were used to infect mouse bone marrow-derived macrophages for various periods at an indicated multiplicity of infection (MOI). Bacteria were deposited onto the macrophages by centrifugation at $150 \times g$ for 5 min at room temperature. After 0-, 5-, 15-, 25-, and 35-min incubations at 37°C, infected macrophages were washed once with medium and were fixed in periodate-lysine-paraformaldehyde (16) containing 5% sucrose for 1 h at 37°C. The samples were washed three times in phosphate-buffered saline (PBS) and wells were successively incubated three times for 5 min in blocking buffer (2% goat serum in PBS) at room temperature. The samples were stained with anti-*B. abortus* polyclonal rabbit serum diluted 1:1,000 in blocking buffer to identify extracellular bacteria. After incubating for 1 h at 37°C, the samples were washed three times for 5 min with blocking buffer, were stained with Cascade blue-conjugated goat anti-rabbit immunoglobulin G diluted 1:500 in blocking buffer, and were incubated for 1 h at 37°C. The samples were washed three times and were mounted in mounting medium. One hundred macrophages were examined per coverslip to determine the total number of intracellular bacteria.

Determination of efficiency of intracellular growth of bacteria. Bacteria were deposited onto macrophages at an MOI of 5 by centrifugation at $150 \times g$ for 5 min at room temperature and then were incubated at 37°C in 5% CO_2 for 1 h. Then the macrophages were washed once with RPMI medium and were incubated with 30 μg/ml gentamicin. At different time points, the cells were washed and lysed with distilled water, and the number of bacteria on plates of a suitable dilution was determined.

Virulence in mice. The virulence was determined by quantitating the survival of the strains in the spleen after 10 days. Mice were injected intraperitoneally with approximately 10^4 CFU of brucellae in 0.1 ml of saline. Groups of five mice were injected with each strain. At 10 days after infection, their spleen was removed, weighed, and homogenized in saline. Tissue homogenates were serially diluted with PBS and were plated on Brucella agar to count the number of CFU in each spleen.

LAMP-1 staining. Infected macrophages were fixed in periodate-lysine-paraformaldehyde–sucrose for 1 h at 37°C and stained for extracellular bacteria as described above. All antibody-probing steps were carried out for 1 h at 37°C. Samples were washed three times in PBS for 5 min and then permeabilized at −20°C in methanol for 10 s. After incubating three times for 5 min with blocking buffer, samples were stained with anti-LAMP-1 rat monoclonal antibody 1D4B diluted 1:100 in blocking buffer (30). After washing three times for 5 min in blocking buffer, samples were stained simultaneously with Texas red-conjugated goat anti-rat immunoglobulin G. Samples were placed in mounting medium and visualized by fluorescence microscopy. Intracellular bacteria were detected by GFP fluorescence and absence of staining with Cascade blue.

Fluorescence labeling of lipid raft-associated molecules. Detection of the localization of GM1 gangliosides with cholera toxin B subunit (CTB) (10 μg/ml), GPI-anchored protein with aerolysin (2.5 μg/ml), and cholesterol with filipin (50 mg/ml) was described previously (33).

RESULTS

Acceleration of bacterial internalization by preloading cholesterol into macrophages. A prominent biological property of acLDL is its ability to induce lipid loading of macrophages in culture, which has been a useful model of the formation of lipid-laden macrophages (Fig. 1) (18, 19, 25). To investigate if intracellular cholesterol affects *B. abortus* internalization into

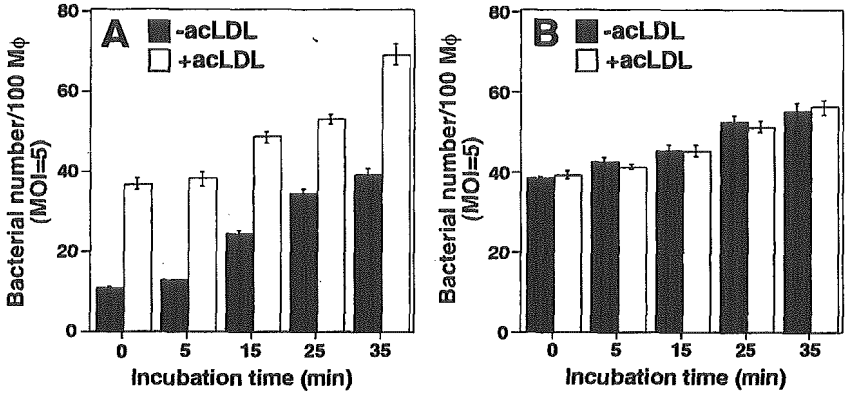

FIG. 2. Internalization of *B. abortus* accelerated by acLDL. Ba600 (wild type) (A) or Ba604 (Δ*virB4*) (B) was deposited onto bone marrow-derived macrophages with (white bars) or without (black bars) acLDL treatment and incubated at 37°C for the periods of time indicated. One hundred macrophages were examined per coverslip. Data are the average of triplicate samples from three identical experiments, and the error bars represent the standard deviation.

macrophages, bacteria were deposited onto macrophages that were preloaded with acLDL, and intracellular bacteria were quantitated microscopically at various times of incubation. The bacteria were deposited onto macrophages by centrifugation, and then Ba604 (Δ*virB4*) was rapidly internalized, with most of the associated bacteria internalized before further incubation at 37°C. In contrast, internalization of Ba600 (wild-type) was delayed and attained the same levels of internalization as Ba604 (Δ*virB4*) only after 25 min of incubation (33). Internalization of Ba600 (wild-type) accelerated by preloading with acLDL into macrophages, but internalization of Ba604 (Δ*virB4*) was not affected (Fig. 2). The percentage of bacteria in macropinosomes did not differ between macrophages treated with and without acLDL (data not shown).

Effects of agents that modulate cholesterol trafficking on bacterial internalization and intracellular replication. Macrophages take up modified lipoproteins by receptor-mediated endocytosis, and then the lipoproteins are delivered to lysosomes for degradation. This cholesterol is believed to mix with the bulk of cholesterol in the plasma membrane. Excess plasma membrane cholesterol then enters the cytoplasm, where the cholesterol is reesterified by ACAT and is stored in cellular lipid droplets (Fig. 1) (19). To investigate if intracellular cholesterol trafficking affects *B. abortus* internalization into macrophages, bacteria were deposited onto macrophages that were pretreated with ACAT inhibitor HL-004, and intracellular bacteria were quantitated microscopically at various times of incubation. HL-004 treatment accelerated the internalization of Ba600 (wild-type) into macrophages preloaded with acLDL (Fig. 3B). Under the same conditions, HL-004 did not accelerate the internalization of Ba604 (Δ*virB4*) (Fig. 3C and D). Macropinosome formation of Ba600 (wild-type) was also enhanced by HL-004 treatment, but the percentage of bacteria in macropinosomes did not differ (data not shown). These results suggest that intracellular cholesterol transport would contribute to VirB-dependent internalization and macropinocytosis of *B. abortus*.

To confirm that plasma membrane cholesterol contributes to *B. abortus* internalization, we tested the effect of ketoconazole, which inhibits cholesterol transport from lysosomes to the cell surface (Fig. 1). Ketoconazole greatly diminished the internalization of Ba600 (wild-type) into macrophages preloaded with or without acLDL (Fig. 3A and B), but under the same conditions, it did not block the internalization of Ba604 (Δ*virB4*) (Fig. 3C and D).

To determine whether intracellular cholesterol trafficking has a role in bacterial replication in macrophages, macrophages were treated with acLDL, ketoconazole, or HL-004 and then were infected with Ba600 (wild type). As reported previously (32, 33), Ba600 (wild-type) replicated in macrophages without ketoconazole treatment, but Ba600 (wild-type) failed to replicate in macrophages treated with ketoconazole (Fig. 3E). Although 12% ± 2.0% of internalized Ba600 (wild type) was observed under ketoconazole treatment (mean ± standard deviation) (Fig. 3A and B), the internalized bacteria did not replicate in the macrophages. Intracellular replication was not affected by acLDL and HL-004 (Fig. 3E). We consistently found that approximately 15% of internalized Ba600 (wild-type) into untreated macrophages target improperly into a LAMP-1 positive compartment (32, 33). These results suggest that other uptake pathways of *B. abortus* by macrophages exist, but replicative phagosome formation requires the uptake pathway associated with plasma membrane cholesterol.

Role of cholesterol trafficking in establishment of *B. abortus* infection. The most prominent cellular feature of Niemann-Pick type C (NPC) disease is lysosomal accumulation of free cholesterol, caused by impaired relocation of cholesterol derived from LDL from the lysosome to other cellular sites, such as the plasma membrane and endoplasmic reticulum (Fig. 1) (23). To investigate if NPC1 contributes to the recruitment of lipid raft-associated molecules, fluorescence-labeled lipid raft-associated molecules, such as cholesterol, GM1 gangliosides, and GPI-anchored proteins, were observed by microscopy. These molecules were in the plasma membrane and intracellular vesicles of macrophages from wild-type mice (Fig. 4). In contrast, these molecules accumulated only in intracellular vesicles in macrophages from NPC1-deficient mice (Fig. 4). Localization of the transmembrane protein CD44, which is not associated with lipid rafts, was not affected by NPC1 (Fig. 4).

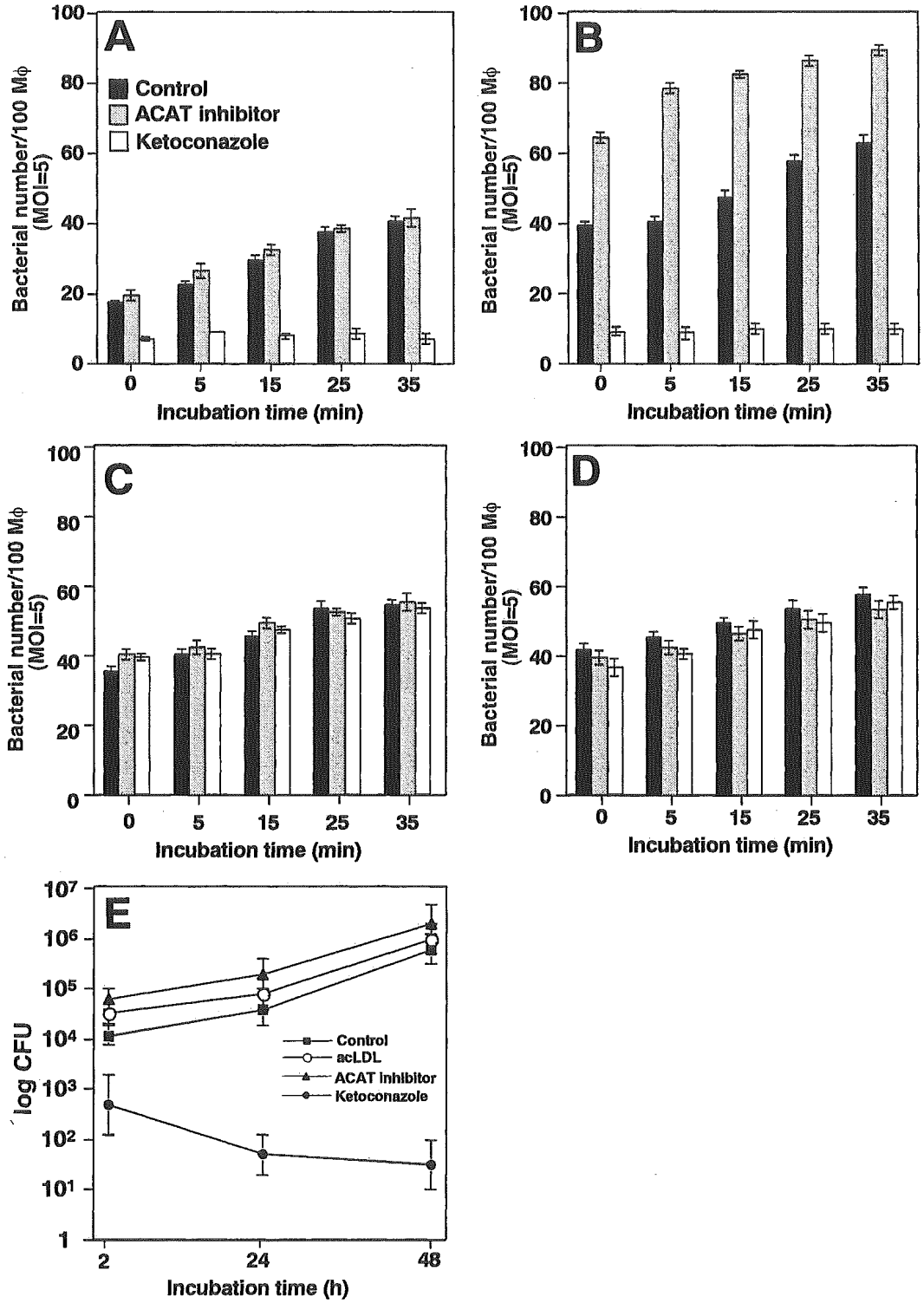

FIG. 3. Internalization of *B. abortus* into macrophages was influenced by plasma membrane cholesterol. Ba600 (wild-type) (A and B) or Ba604 (Δ*virB4*) (C and D) was deposited onto bone marrow-derived macrophages with ketoconazole (white bars) or with ACAT inhibitor HL-004 (gray bars), or without drug treatment (black bars) in the presence (B and D) or absence (A and C) of acLDL and incubated at 37°C for the periods of time indicated. One hundred macrophages were examined per coverslip. Data are the average of triplicate samples from three identical experiments, and the error bars represent the standard deviation. (E) Ketoconazole inhibited intracellular replication of *B. abortus* in macrophages. Macrophages in the presence or absence of ketoconazole, ACAT inhibitor HL-004, or acLDL were infected with Ba600 (wild type) as described in Materials and Methods. Data points and error bars represent the mean CFU of triplicate samples from a typical experiment (performed at least four times) and their standard deviation, respectively.

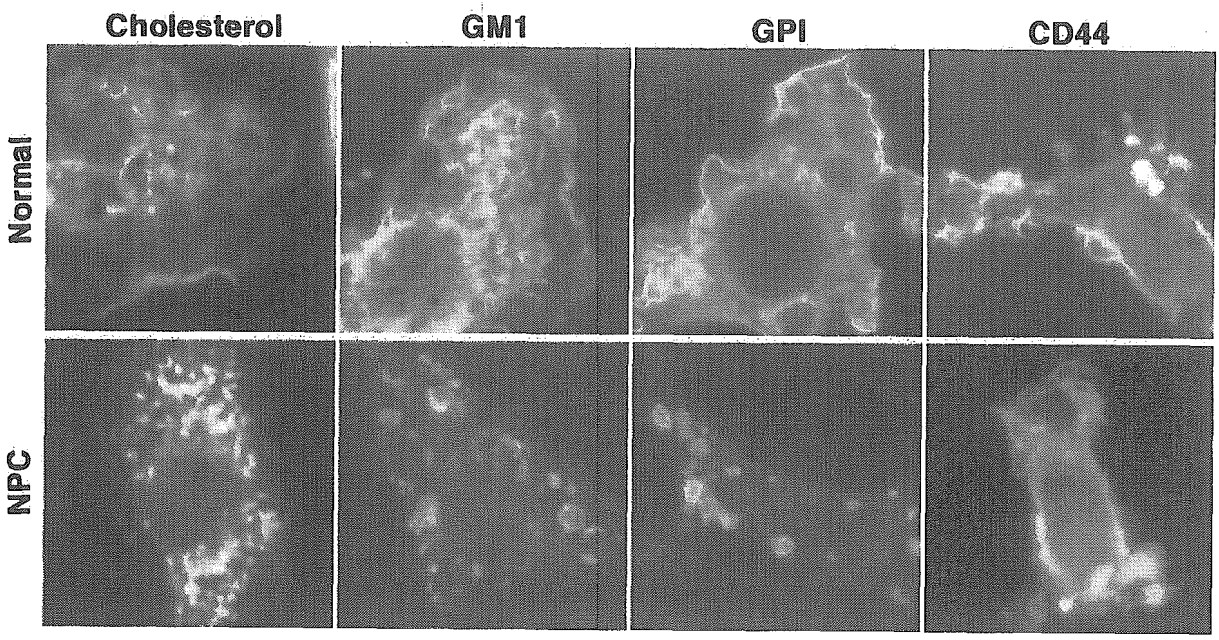

FIG. 4. Intracellular distribution of lipid raft-associated molecules in NPC1-deficient macrophages. Macrophages of wild-type (upper panels) or NPC1-deficient (lower panels) mice were labeled with indicated molecules.

These results suggest that NPC1 influences lipid raft formation on the macrophage surface.

We next investigated if NPC1 contributes to the internalization and intracellular replication of *B. abortus*. *B. abortus* was infected to bone marrow derived-macrophages from wild-type or NPC1-deficient BALB/c mice, and the intracellular bacteria were quantitated microscopically at various periods of incubation. Macrophages from wild-type mice supported internalization and intracellular replication of Ba600 (wild-type), but not macrophages from NPC1-deficient mice (Fig. 5A). Fewer bacteria were internalized in macrophages from NPC1-deficient mice, but they did not replicate in the macrophages (Fig. 5C). Macrophages from wild-type and NPC1-deficient mice showed no significant difference in the internalization of Ba604 (Δ*virB4*) (Fig. 5B). In NPC1-deficient mice, Ba600 (wild-type) failed to block phagosome maturation, as shown by colocalization of phagosomes containing the bacteria and the late endocytic marker, LAMP-1, at 1 h after infection (82.8% ± 3.4% positive) (Fig. 6B and D). In contrast, Ba600 (wild-type) prevented phagosome-lysosome fusion, and therefore phagosomes containing Ba600 (wild-type) do not have endocytic and lysosomal marker proteins in macrophages from wild-type mice (Fig. 6A and C). These results suggest that replicative phagosome formation required uptake pathway associated with NPC1.

To find if this defect in internalization and intracellular replication of *B. abortus* correlates with an inability to establish infection in the host, we experimentally infected wild-type or NPC1-deficient mice with *B. abortus*. Many bacteria were recovered from the spleen of wild-type mice infected with Ba600 (wild type) at 10 days after infection, but fewer bacteria were recovered from NPC1-deficient mice, based on the number of CFU in each spleen (Fig. 5D). These results indicated that *B. abortus* proliferation was promoted by NPC1.

DISCUSSION

In this study we showed that internalization and intracellular replication of *B. abortus* in mouse macrophages are influenced by plasma membrane cholesterol and that intracellular cholesterol trafficking is essential to establish *B. abortus* infection in the mouse model. These events were dependent on the presence of the VirB system. Studies of the cellular trafficking of cholesterol derived from the metabolism of LDL showed that after hydrolysis of LDL cholesteryl ester in lysosomes, most LDL-derived cholesterol traffics to the plasma membrane (14). The internalization of *B. abortus* into macrophages was accelerated by preloading with acLDL, indicating that the cholesterol on the plasma membrane of macrophages contributes to the internalization of *B. abortus*. To confirm this possibility, we used two inhibitors of intracellular cholesterol trafficking, HL-004 and ketoconazole. As HL-004 is a specific ACAT inhibitor (18), alterations in cholesterol metabolism by HL-004 can be attributed to the intracellular ACAT inhibition in macrophages (19). Macrophages incorporate modified LDL via scavenger receptors, which is not down-regulated by cellular sterol levels (8). The incorporated cholesteryl ester is delivered to lysosomes, and is hydrolyzed to free cholesterol, which forms the intracellular free cholesterol pool. Excess free cholesterol is esterified by ACAT and the cholesteryl ester is stored in cytoplasmic inclusions. This cholesteryl ester is the substrate for neutral cholesteryl ester hydrolase. Thus, a cholesteryl ester cycle of de-esterification exists because of the hydrolase and reesterification by ACAT. Free cholesterol can move between intracellular pools and the plasma membrane (3). Internalization and intracellular replication of *B. abortus* in macrophages were modulated by cholesterol-rich microdomains, so-called lipid rafts, on plasma membrane surfaces (33). As the cholesterol microdomains are induced in macrophages when esteri-

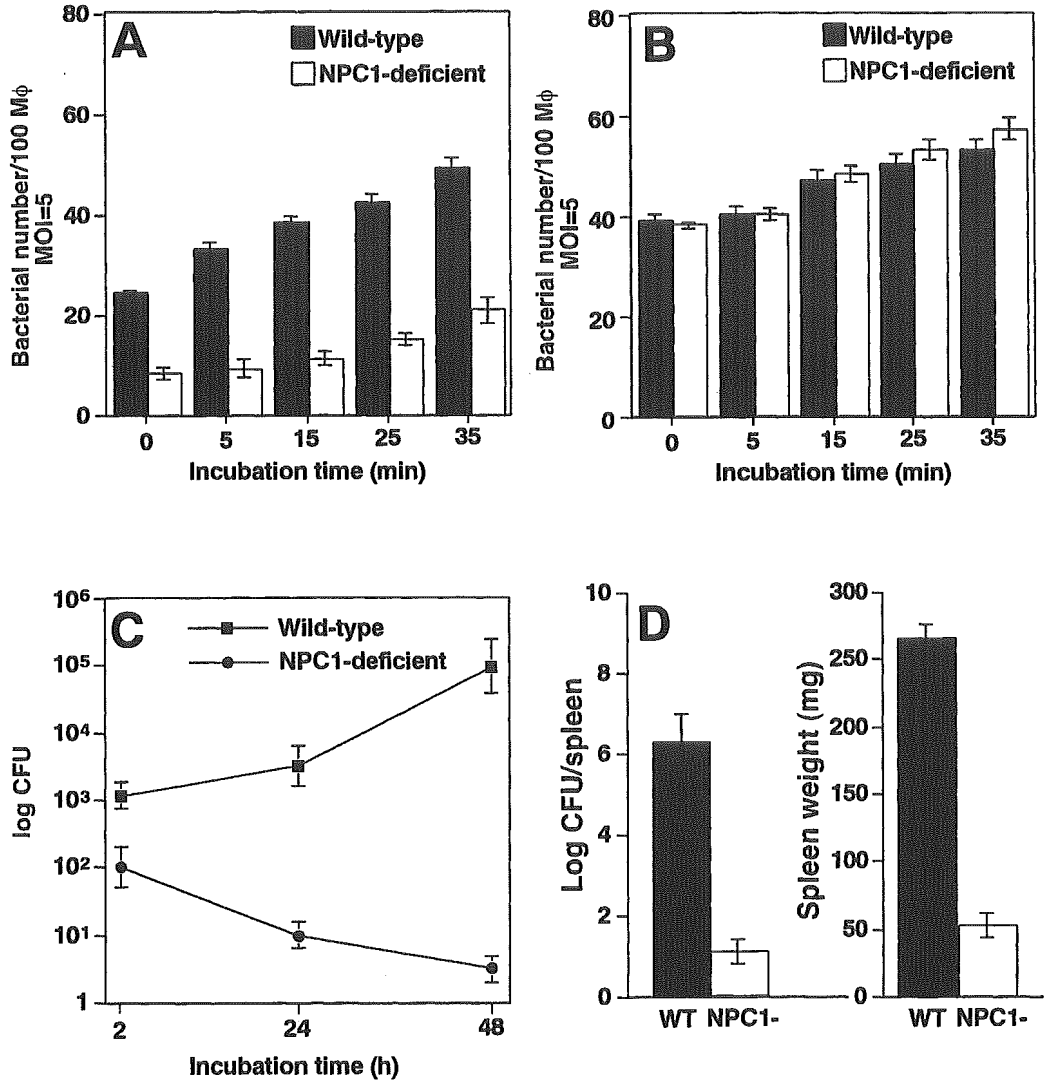

FIG. 5. NPC1-influenced *B. abortus* infection. (A and B) Internalization of *B. abortus*. Macrophages from wild-type (black bars) or NPC1-deficient (white bars) mice were infected with virulent Ba600 (wild type) (A) or Ba604 (Δ*virB4*) (B) for the periods of time indicated. Data are the average of triplicate samples from three identical experiments, and the error bars represent the standard deviation. (C) Intracellular replication of *B. abortus*. Macrophages from wild-type or NPC1-deficient mice were infected with Ba600 (wild type). Data points and error bars represent the mean CFU of triplicate samples from a typical experiment (performed at least four times) and their standard deviation, respectively. (D) Proliferation in mice. Wild-type (black bar) or NPC1-deficient (white bars) mice were infected with virulent *B. abortus*. Recovery of viable bacteria from the spleen and the weights of spleens of infected mice at 10 days postinfection are shown. Error bars indicate standard deviations.

fication of excess LDL-derived cholesterol is blocked with ACAT inhibitor (10), the internalization of *B. abortus* by uptake pathway associated with lipid rafts into macrophages increased by ACAT inhibitor treatment. In contrast, ketoconazole treatment greatly diminished the internalization of *B. abortus* into macrophages. Ketoconazole interferes with trafficking of cholesterol from lysosomes to the plasma membrane (12). As the appearance of cholesterol microdomains can be inhibited by ketoconazole (10), the internalization of *B. abortus* by uptake pathway associated with lipid rafts into macrophages decreases upon ketoconazole treatment. These results suggest that the plasma membrane cholesterol should influence the internalization of *B. abortus*. Fewer *B. abortus* cells were internalized into macrophages treated with ketoconazole, but the internalized bacteria did not replicate, suggesting that replicative phagosome formation would require correct intracellular cholesterol trafficking and plasma membrane cholesterol.

To confirm this hypothesis, macrophages from NPC1-deficient mice were infected with *B. abortus*. The gene that causes NPC disease, referred to as *NPC1*, has been mapped to a region of chromosome 18 in both humans and mice and has been cloned (15). Although the function of NPC1 remains undefined, studies have shown a crucial role for this protein in cholesterol metabolism (13). NPC1-deficient mice share many of the pathophysiological abnormalities observed in patients with NPC, including accumulation of cholesterol in tissues (15). Our results showed that lipid raft-associated molecules accumulate in intracellular vesicles in macrophages from

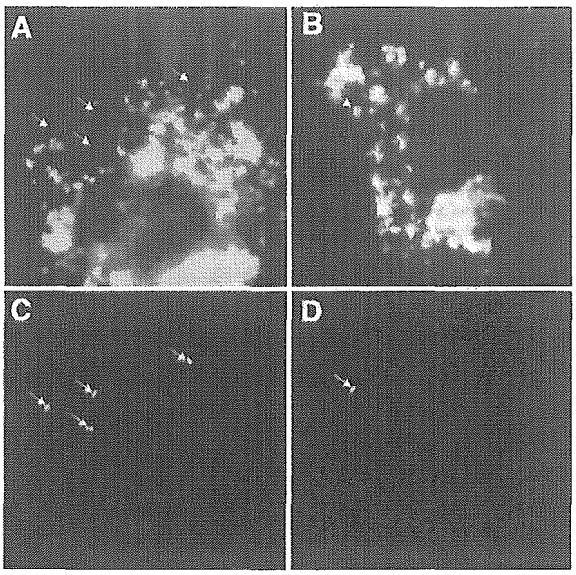

FIG. 6. Colocalization of *B. abortus* with late endosomal and lysosomal marker LAMP-1 in macrophages from NPC1-deficient mice by immunofluorescence microscopy. Macrophages from wild-type mice (A and C) or NPC1-deficient mice (B and D) were infected with Ba600 (wild type) for 1 h, fixed, and stained for LAMP-1 colocalization (A and B) and intracellular bacteria (C and D). Arrows point to bacteria.

NPC1-deficient mice. NPC1 is recruited to the site of free cholesterol accumulation by enrichment of cellular cholesterol or by pharmacological intervention of cholesterol egress from the lysosomes (34). Intracellular trafficking of GM1 ganglioside in NPC1-deficient Chinese hamster ovary cells has been shown by using CTB as a probe (29). CTB-labeled vesicles contain the early endosome marker Rab5 but not LAMP-2, indicating that they represent early endosomes. Similarly, CTB accumulate in intracellular vesicles of human NPC fibroblasts that contain both Rab5 and early endosomal antigen 1 (29). Presumably, these results, together with our results, indicate that cholesterol or GM1 ganglioside accumulate in lysosomes or early endosomes in macrophages from NPC1-deficient mice. Therefore, the internalization of *B. abortus* by uptake pathway associated with lipid rafts was inhibited in macrophages from NPC1-deficient mice.

The role of mouse macrophages in mediating resistance or susceptibility among mouse strains to some intracellular pathogens has been shown by studies of the *Ity/Lsh/Bcg* resistance model; resistance to *Salmonella enterica* serovar Typhimurium, *Leishmania donovani*, and mycobacterial species is regulated by the polymorphism of the *Nramp1* gene that controls macrophage function (6). Bovine Nramp1 is a major candidate for controlling the in vivo resistant phenotype against *B. abortus* infection (2). Our results indicate that NPC1 promotes the internalization and intracellular replication of *B. abortus* and also contributes to bacterial proliferation in mice. However, control of *B. abortus* infections is a multigenic trait (9), and further investigation is needed to clarify the genetic control of *B. abortus* infection.

Cholesterol or GPI-anchored proteins is included in apicomplexan *Toxoplasma gondii* and *Plasmodium falciparum* vacuoles (11, 17). Cholesterol is essential for the uptake of *Mycobacterium bovis* by macrophages (7). Cholesterol accumulates at the site of *M. bovis* entry, depleting plasma membrane cholesterol specifically inhibits *M. bovis* uptake, and *M. bovis* has a high binding capacity for cholesterol (7). Macropinosomes harboring *L. pneumophila* also include lipid raft-associated macromolecules (31). A similar process of selective lipid recruitment has been described during human immunodeficiency virus or influenza virus budding from mammalian cells (22, 26). Since lipid rafts are thought to be involved in signaling pathways in immune cells, uptake processes associated with lipid rafts might lead microorganisms into compartments that avoid fusion with the lysosomal network, and that is essential for the establishment of infection. The results of this study will provide a new target of prevention against infection by intracellular pathogens.

ACKNOWLEDGMENTS

This work was supported, in part, by grants-in-aid for scientific research (12575029 and 13770129), Japan Society for the Promotion of Science, and by the Sasakawa Scientific Research Grant from The Japan Science Society.

REFERENCES

1. **Baldwin, C. L., and A. J. Winter.** 1994. Macrophages and *Brucella*. Immunol. Ser. **60:**363–380.
2. **Barthel, R., J. Feng, J. A. Piedrahita, D. N. McMurray, J. W. Templeton, and L. G. Adams.** 2001. Stable transfection of the bovine *NRAMP1* gene into murine RAW264.7 cells: effect on *Brucella abortus* survival. Infect. Immun. **69:**3110–3119.
3. **Brown, M. S., Y. K. Ho, and J. L. Goldstein.** 1980. The cholesteryl ester cycle in macrophage foam cells: continual hydrolysis and re-esterification of cytoplasmic cholesteryl esters. J. Biol. Chem. **255:**9344–9352.
4. **Christie, P. J., and J. P. Vogel.** 2000. Bacterial type IV secretion: conjugation systems adapted to deliver effector molecules to host cells. Trends Microbiol. **8:**354–360.
5. **Comerci, D. J., M. J. Martinez-Lorenzo, R. Sieira, J. Gorvel, and R. A. Ugalde.** 2001. Essential role of the VirB machinery in the maturation of the *Brucella abortus*-containing vacuole. Cell. Microbiol. **3:**159–168.
6. **Forbes, J. R., and P. Gros.** 2001. Divalent-metal transport by NRAMP proteins at the interface of host-pathogen interactions. Trends Microbiol. **9:**397–403.
7. **Gatfield, J., and J. Pieters.** 2000. Essential role for cholesterol in entry of mycobacteria into macrophages. Science **288:**1647–1650.
8. **Goldstein, J. L., Y. K. Ho, S. K. Basu, and M. S. Brown.** 1979. Binding site on macrophages that mediates uptake and degradation of acetylated low density lipoprotein, producing massive cholesterol deposition. Proc. Natl. Acad. Sci. USA **76:**333–337.
9. **Ho, M., and C. Cheers.** 1982. Resistance and susceptibility of mice to bacterial infection. IV. Genetic and cellular basis of resistance to chronic infection with *Brucella abortus*. J. Infect. Dis. **146:**381–387.
10. **Kruth, H. S., I. Ifrim, J. Chang, L. Addadi, D. Perl-Treves, and W.-Y. Zhang.**2001. Monoclonal antibody detection of plasma membrane cholesterol microdomains responsive to cholesterol trafficking. J. Lipid Res. **42:** 1492–1500.
11. **Lauer, S., J. VanWye, T. Harrison, H. McManus, B. U. Samuel, N. L. Hiller, N. Mohandas, and K. Haldar.** 2000. Vacuolar uptake of host components, and a role for cholesterol and sphingomyelin in malarial infection. EMBO J. **19:**3556–3564.
12. **Liscum, L.** 1990. Pharmacological inhibition of the intracellular transport of low-density lipoprotein-derived cholesterol in Chinese hamster ovary cells. Biochim. Biophys. Acta **1045:**40–48.
13. **Liscum, L., and J. J. Klansek.** 1998. Niemann-Pick disease type C. Curr. Opin. Lipidol. **9:**131–135.
14. **Liscum, L., and N. J. Nunn.** 1999. Intracellular cholesterol transport. Biochim. Biophys. Acta **1438:**19–37.
15. **Loftus, S. K., J. A. Morris, E. D. Carstea, J. Z. Gu, C. Cummings, A. Brown, J. Ellison, K. Ohno, M. A. Rosenfeld, D. A. Tagle, P. G. Pentchev, and W. J. Pavan.** 1997. Murine model of Niemann-Pick C disease: mutation in a cholesterol homeostasis gene. Science **277:**232–235.
16. **McLean, I. W., and P. K. Nakane.** 1974. Periodate-lysine-paraformaldehyde fixative: a new fixative for immunoelectron microscopy. J. Histochem. Cytochem. **22:**1077–1083.
17. **Mordue, D. G., N. Desai, M. Dustin, and L. D. Sibley.** 1999. Invasion by *Toxoplasma gondii* establishes a moving junction that selectively excludes